Design of a Model for the Measurement of the Pressure Distribution on an Axially Symmetric Rotating Body

Thesis by

Harold C. Larsen

In Partial Fulfillment of the Requirements

for the Degree of

Aeronautical Engineer

California Institute of Technology

Pasadena, California

1955

ACKNOWLEDGEMENTS

The author is indebted to Drs. C. B. Millikan and A. Roshko for their encouragement and supervision of the work, especially the helpful criticism of designs presented in the evolution of the model. Dr. A. Klein offered advice and suggestions useful in the design of scientific apparatus, and Messers. W. Sublette and W. Runner of the Galcit Machine Shop patiently endured the author's many questions on machining techniques and suggested improvements to simplify the construction.

ABSTRACT

Two simplified theories for the corrections to be applied to the measured pressure in order to determine the pressure distribution on a rotating body are presented. One is based on continuous sampling, and the other is based upon pulse sampling. The problems associated with and the design features of systems using different pressure sensing elements are reviewed. From these considerations, the system offering the simplest solution is selected. The design features and compromises of a model designed and constructed utilizing pulse sampling are discussed.

TABLE OF CONTENTS

INTRODUCTION

The two dimensional ideal fluid flow past a circular cylinder with circulation is well known. This flow gives rise to a net force at right angles to the direction of the free stream velocity vector, and has been used as a model to describe the "Magnus Effect". The curvilinear motion of a spin stabilized projectile along a trajectory has a cross flow component of velocity similar to the classical two dimensional flow around a circular cylinder with circulation, and has been used to explain why a spin stabilized projectile drifts from the plane in which it was fired. Experience with artillery shells and tests on spinning missiles has shown that for small angles of yaw, a spinning axially symmetrical body has aerodynamic moments which tend to damp out any yawing tendencies, but at some critical angle of yaw destabilizing moments occur which can cause erratic flight path behavior. This characteristic has been observed with aerial bombs, mortars, artillery shells, and other ordnance. It has become of importance that, with the use of rocket propelled missiles as aerodynamic testing equipment, more detailed information be obtained on this characteristic.

Efforts to obtain more knowledge of the causes for the erratic behavior and abrupt change in moment characteristics of spinning missiles had been confined to net force and moment characteristics obtained from wind tunnel balance measurements. These tests yield gross information applicable to one particular model, but give no information of the detailed behavior. Kelly (1) has developed a theory for the influence of an attached boundary layer on the "Magnus force and moment" of slender bodies in which the nose and tail effect may be neglected.

This theory can treat small angles of yaw, but is invalid as soon as separation occurs. To be of greatest value, the circumferential and axial pressure gradients on the body should be known. As a first approximation, classical theory may be used to approximate these pressure gradients.

The current Galcit investigation of the Magnus Effect and the transition of boundary layers on spinning missiles indicated the need of detailed information of the pressure distribution on spinning bodies. This, in addition to the desire to obtain information of the cause of the erratic behavior at large angles of yaw, resulted in the initiation of an investigation of the problems associated with, and the feasibility of designing, a model capable of yielding qualitative and quantitative pressure distribution data. Several methods were investigated, and the direct measurement of the static pressure by pulse sampling was selected as the one having greatest promise of success. This paper is concerned with the design of such a model.

LIST OF SYMBOLS

A - area

D - pressure transmitting tube diameter, model diameter

d - orifice diameter

j - $\sqrt{-1}$ imaginary number

K($\dot{\phi}$) - ratio peak pulse pressure to average measured pressure at any given angular velocity

L - length of pressure transmitting tube

M - Mach Number

n - polytropic exponent, number of orifices on perimeter

p - pressure

Q - volume rate of flow

R - gas constant

r - radius

V - instrument volume

v - velocity

T - temperature, time between pulses

$T\frac{1}{2}$ - relaxation time

γ - ratio of specific heats, adiabatic exponent

δ_o - phase angle

λ_o - characteristic time

λ - decay constant

μ - coefficient of viscosity

ξ - nondimensional pressure fluctuation

ρ - density

τ - time

$\dot{\phi}$ - angular velocity-radians per second

χ - complex attenuation factor

ω - circular frequency of pressure variation

subscripts

a - ambient

I - instrument

m - measured

o - outer surface

t - tangential

Part I -- THEORY

A - ATTENUATION OF OSCILLATORY PRESSURES IN INSTRUMENT LINES UNDER THE INFLUENCE OF A RADIAL ACCELERATION.

Any pressure measuring device situated in a rotating body will not indicate the true pressure at the surface of the body because of the influence of the radial acceleration and the attenuation of any pressure fluctuations due to the action of viscosity in the pressure transmitting tube, and the dissipation of the pressure signal in the instrument volume. There will be a phase relation between the fluctuation of the pressure measured at the instrument, and the pressure fluctuation at the point on the surface of the body. An elementary analysis reveals the fundamental features of these effects.

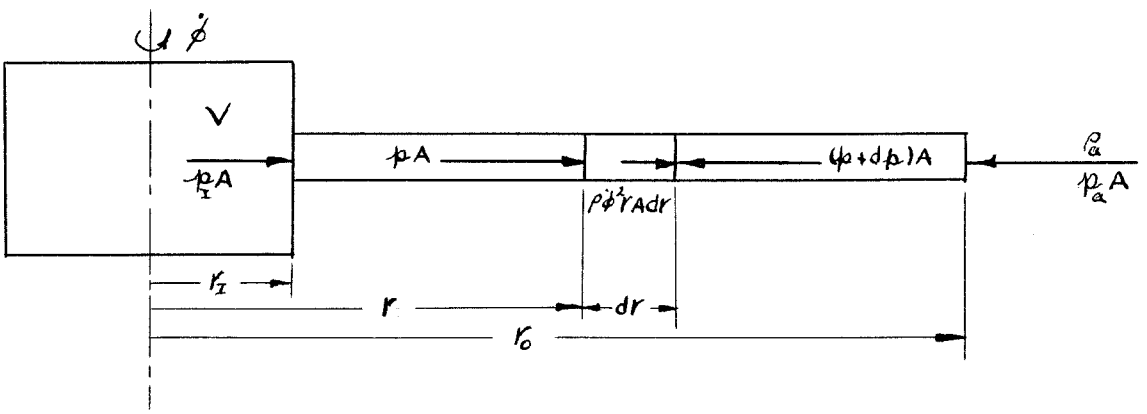

Fig. 1

Assume a small cylinder is rotating at constant angular velocity, $\dot{\phi}$, about an axis perpendicular to its generating axis as shown in figure 1, and connects an instrument of volume, V, at instrument pressure, p_I, with the atmosphere at ambient pressure, p_a. Assume that static equilibrium has been attained under the applied forces which are assumed to be only the pressure forces and the inertial reaction. The differential equation for the pressure at any point along the tube is

$$dp = \rho \dot{\phi}^2 r dr \qquad (1)$$

with the boundary conditions:

$p = p_I$ at $r = r_I$; $p = p_a$ at $r = r_o$.

The solution of this equation for incompressible, isothermal, polytropic, and adiabatic assumptions for the functional relation between the pressure and the density are:

$$\frac{p}{p_a} = 1 - \frac{\rho_a \dot{\phi}^2 r_o^2 \left[1 - (r_I/r_o)^2\right]}{p_a} \qquad (2a) \qquad \text{incompressible}$$

$$\frac{p}{p_a} = e^{\frac{-\dot{\phi}^2 r_o^2 \left[1 - (r_I/r_o)^2\right]}{2RT}} \qquad (2b) \qquad \text{isothermal}$$

$$\frac{p}{p_a} = \left[1 - \frac{(n-1)\rho_a \dot{\phi}^2 r_o^2 \left\{1 - (r_I/r_o)^2\right\}}{2n\, p_a}\right]^{\frac{n}{n-1}} \qquad (2c) \qquad \text{polytropic}$$

$$\frac{p}{p_a} = \left[1 - \frac{(\gamma-1)}{2} M_t^2 \left\{1 - (r_I/r_o)^2\right\}\right]^{\frac{\gamma}{\gamma-1}} \qquad (2d) \qquad \text{adiabatic}$$

where $\dot{\phi}^2 r_o^2 = v_t^2$; $\gamma p_a/\rho_a = a_a^2$; and $v_t^2/a_a^2 = M_t^2$.

Equations (2) relate the pressure at any point in the tube with the ambient pressure for various thermodyanmic assumptions. Equation (2a) is the familiar parabolic variation of pressure with radius ratio for an incompressible fluid. Equation (2b) assumes an isothermal relation for the gas in the pressure transmitting tube, and shows that if under equilibrium conditions heat should be transferred to the tube, for example from the driving motor, the pressure indicated by the instrument would decrease.

Equation (2c) shows a similar relation for polytropic conditions in the tube. These conceivably may exist if heat is conducted along the walls of the tube from hot spots in the device. Equation (2d) shows a similar relation for adiabatic conditions in the tube. This is the case which would most likely exist, especially if strong pressure gradients exist along the tube. If it is assumed that adiabatic conditions do exist in the tube, and the pressure ratio is calculated for various radius ratios and tangential or rotational Mach Numbers, figures 2 and 3 result. Figure 2 shows the effect of radius ratio at constant tangential Mach Number, and figure 3 shows the effect of tangential Mach Number at constant radius ratio. These curves show the desirability of maintaining as high a radius ratio as possible, and as low a tangential Mach Number as possible. The design conditions for the model constructed correspond to a radius ratio of 0.866, and a maximum tangential Mach Number of 0.07. With these design conditions, one can safely assume an incompressible fluid in the pressure transmitting tube. This assumption greatly simplifies the following analysis for the effect of viscous attenuation.

A simplified analysis of the response of the system to a fluctuating pressure was made following the method in reference (2). The system is assumed to consist of a rigid volume representing the instrument, a constant diameter pressure transmitting tube of length $L = (r_o - r_I)$ and of area A. A sinusoidally fluctuating pressure, $\Delta p = \Delta p_o e^{j\omega t}$, is assumed to be applied at the entrance to the tube. An incompressible fluid is assumed, and entrance effects are neglected. Viscosity is assumed to retard any flow in and out of the tube, and Poiseuille flow is assumed to apply in the tube.

VARIATION OF PRESSURE RATIO WITH RADIUS RATIO AT SEVERAL TANGENTIAL MACH NUMBERS

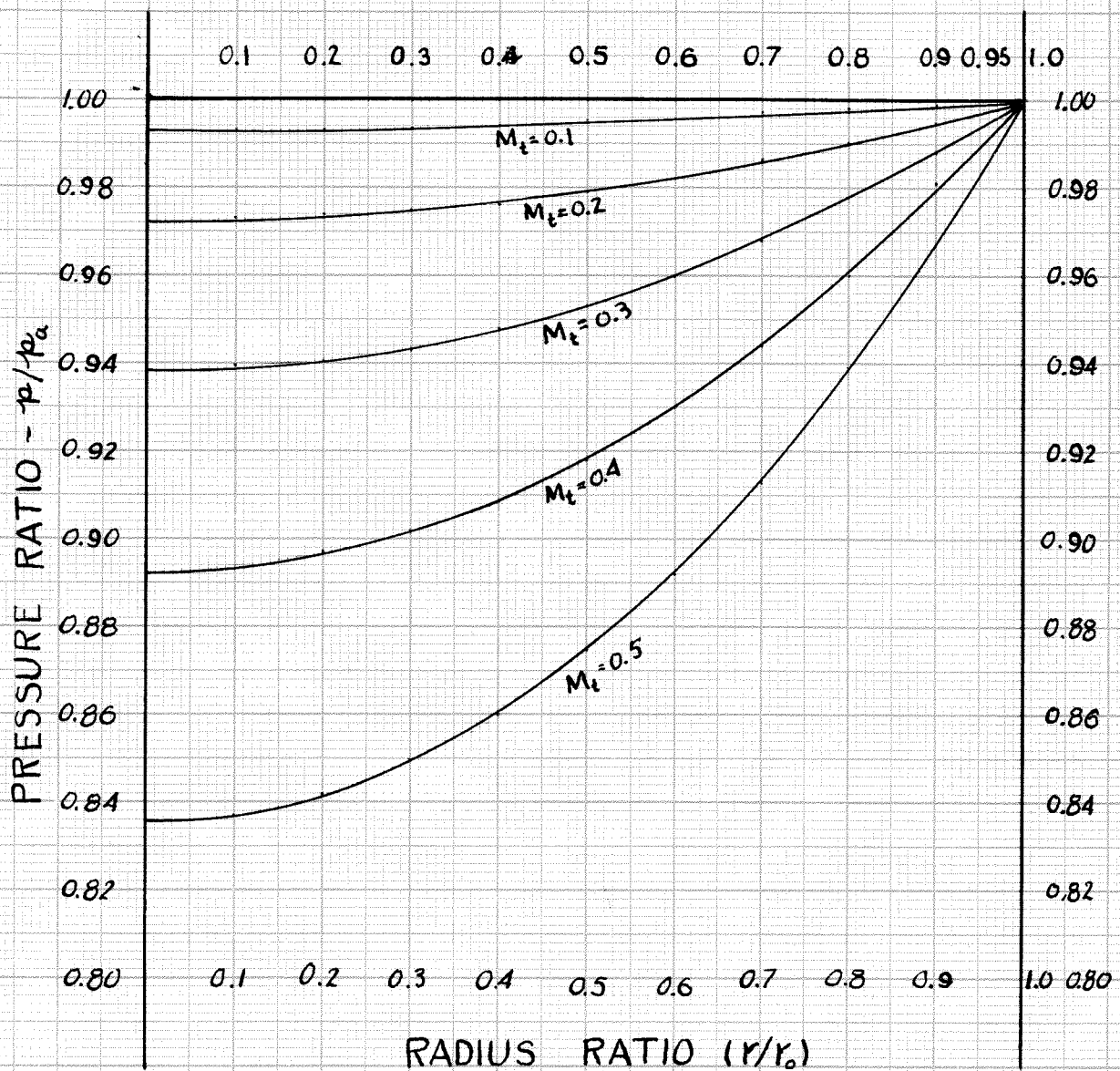

Fig. 2

VARIATION OF PRESSURE RATIO WITH TANGENTIAL MACH NUMBER AT SEVERAL RADIUS RATIOS

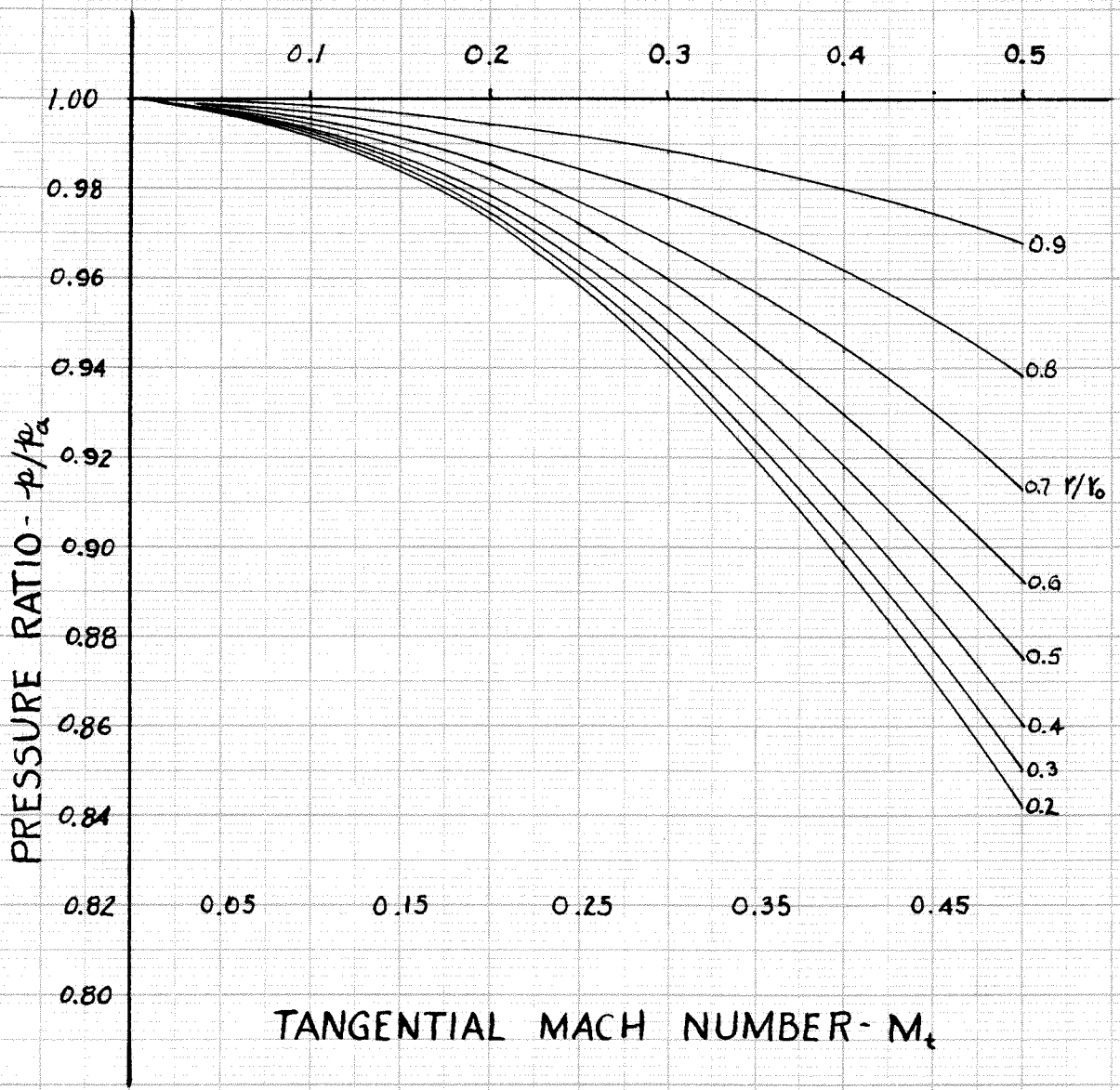

Fig. 3

An isothermal compression and expansion is assumed to occur as fluid flows into and out of the instrument volume, V. The equations of motion become with these assumptions:

$$\frac{\partial p}{\partial r} = \rho_a \dot{\phi}^2 r + \frac{128\mu Q}{\pi D^4} \qquad (3) \qquad \text{Poiseuille flow}$$

$$\frac{\partial(\rho Q)}{\partial t} = -A\frac{\partial \rho}{\partial t} \qquad (4) \qquad \text{continuity}$$

Using the assumption of an incompressible fluid, that is, the fluid in the tube moves like a piston, one obtains upon eliminating Q and differentiating (3) with respect to r,

$$\frac{\partial^2 p}{\partial r^2} = \rho \dot{\phi}^2 \qquad (5)$$

for conditions along the tube. The boundary conditions are

$$p = p_a + \Delta p_o e^{j\omega t} \quad \text{at } r = r_o \qquad (6)$$

$$Q = \frac{V}{p_I}\frac{\partial p}{\partial t} \qquad \frac{\partial p}{\partial r} = \rho \dot{\phi}^2 r + \frac{128\mu Q}{\pi D^4} \quad \text{at } r = r_I \qquad (7)$$

Equation (6) states that there is a sinusoidal variation of pressure about the mean ambient pressure at the surface.

The first line of equation (7) expresses the fact that the compression of the fluid in the instrument is due to flow in, while the second line states that the rate of flow into the instrument is limited by the pressure gradient at the entrance to the instrument volume from the tube. Using $Q = \frac{V}{p_I}\frac{\partial p}{\partial t}$, this may be put into the following form:

$$\frac{\partial p}{\partial r} = \rho \dot{\phi}^2 r + \frac{128\mu V}{p_I \pi D^4}\frac{\partial p}{\partial t} = \rho \dot{\phi}^2 r + \frac{32\mu}{L p_I}\left(\frac{L}{D}\right)^2\left(\frac{V}{AL}\right)\frac{\partial p}{\partial t} = \rho \dot{\phi}^2 r + \frac{\lambda_o}{L}\frac{\partial p}{\partial t} \qquad (8)$$

where

$$\lambda_o = \frac{32\mu}{p_I}\left(\frac{L}{D}\right)^2\left(\frac{V}{AL}\right) = \frac{32\mu}{p_a - \frac{\rho\dot{\phi}^2 r_o^2}{2}\left[1 - (r_I/r_o)^2\right]}\left(\frac{L}{D}\right)^2\left(\frac{V}{AL}\right) \qquad (9)$$

which has the dimension of time, and may be considered the time constant for the system. This is seen to depend upon the rotational velocity $\dot{\phi}$ for a rotating body.

The equation can be non-dimensionalized by considering the local percentage of pressure fluctuation from the mean. Define:

$$\xi = \frac{p - \left\{p_a - \rho\dot{\phi}^2 r_o^2\left[1 - (r/r_o)^2\right]\right\}}{p_a} \qquad (10)$$ and assume

$$\xi = \bar{\xi}\, e^{j\omega t} \qquad (11)$$

where $\bar{\xi}$ is a space dependent variable and is the maximum amplitude at a point and $e^{j\omega t}$ is the time dependent part. The equations become

$$\frac{d^2\bar{\xi}}{dr^2} = 0 \qquad (12)$$

$$\bar{\xi} = \xi_o \qquad \text{at } r = r_o \qquad (13), \text{ and}$$

$$\frac{d\bar{\xi}}{dr} = \frac{\lambda_o\omega}{L}\bar{\xi}j \qquad \text{at } r = r_I \qquad (14).$$

The solution of equation (12) which satisfies equations (13) and (14) is given by

$$\bar{\xi} = \left\{\frac{1 + j\lambda_o\left[1 - (r_o - r)/(r_o - r_I)\right]}{1 + j\lambda_o\omega}\right\}\xi_o \qquad (15)$$

The ratio of the amplitude of the pressure fluctuation at the instrument to that at the surface of the rotating body is

$$\frac{\bar{\xi}_{r_I}}{\xi_o} = \frac{1}{1 + j\lambda_o\omega} = \frac{1}{1 + \chi_o j} \qquad (16), \qquad \text{where}$$

$$\chi_o = \lambda_o\omega \qquad (17).$$

The real part of equation (16) is the attenuation of the pressure fluctuation, and the imaginary part is the phase lag. That is,

$$\left| \frac{\overline{\xi}_{\mu_1}}{\xi_o} \right| = \frac{1}{[1 + (\lambda_o \omega)^2]^{\frac{1}{2}}} \qquad (18)\ ,\ \text{where}$$

$$\tan \delta_o = \chi_o$$

$$\lambda_o = \frac{32\left(\frac{L}{D}\right)^2 \left(\frac{V}{AL}\right)\mu_o}{\left\{p_a - \rho_a \frac{\dot{\phi}^2 r_o^2}{2}\left[1 - (r_I/r_o)^2\right]\right\}}$$

$$\tan \delta_o = \frac{32\left(\frac{L}{D}\right)^2 \left(\frac{V}{AL}\right)\mu_o \omega}{\left\{p_a - \rho_a \frac{\dot{\phi}^2 r_o^2}{2}\left[1 - (r_I/r_o)^2\right]\right\}} \qquad (19)\ .$$

Equation (18) shows the attentuation increases with angular frequency of the applied fluctuation, the speed of rotation, and a decrease of the radius ratio. It also shows the desirability of maintaining a short pressure transmitting tube, and achieving a small instrument volume to pressure transmitting tube ratio. The phase lag is similarly affected. Large tube diameters are desirable in any given design, but in a rotating body, this conflicts with the use of small tube diameters to measure pressure over a small subtended arc length in order to localize the pressure measuring area and increase the angular sensitivity of the instrument.

In principle, the response of the system to a square wave can be found from the response to a sine wave by Fourier analysis. This was not done, since the essential features of the problem are believed to be revealed by the above analysis. In reference (2) the high quality response of a pressure measuring system was calculated using a refined theory in which first order corrections for compressibility of the gas and harmonic distortion were included.

High quality transmission is defined in reference (2) as an attenuation ratio of 1 ± 0.05 or 30° phase lag whichever was less.

Table I gives the results which bound the design operating conditions for the proposed model. The tube used in this computation was 0.1 in. ID with an A = 0.0079 sq. in. Instrument volumes of 0.1 in^3 and 1 in^3 were used in the calculation.

TABLE I

$V = 0.1\ in^3$						$V = 1\ in^3$					
ω	L	L/D	V/AL	$\lvert\xi_{x_1}/\xi_o\rvert$	δ_o	ω	L	L/D	V/AL	$\lvert\xi_{x_2}/\xi_o\rvert$	δ_o
20π	48"	480	11	1.05	4^o	20π	12"	120	110	1.05	--
200π	15"	150	9.9	1.05	--	200π	---	---	---	-----	--

The column headed L is the maximum length of tubing which would give high quality transmission with the assumed instrument volumes at angular frequencies of 20π and 200π radians per second. The calculations are based on nondimensionalized curves, and the data have been reduced to show the allowable length of tube to tube diameter and instrument volume to tube volume. The two instrument volumes and two angular frequencies show the allowable limits on (L/D) and (V/AL) for high quality transmission. It is seen that the amplitude ratio $\lvert\xi_{x_1}/\xi_o\rvert$ controls these ratios. These calculations include first order effects of compressibility and harmonic distortion. It is for these reasons that the amplitude ratio is greater than unity. It is seen that phase angle, δ_o, is small or negligible. The expected range of frequencies in the model are 20π to 200π radians per second. The (L/D) ratio of the pressure transmitting tube in the model is 8, therefore to attain high quality the (V/AL) ratio will be the controlling factor.

These results emphasize the necessity of maintaining small instrument volumes and short pressure transmitting tubes, especially as the angular frequency of the fluctuations is increased.

On the proposed model the angular frequency is essentially $\dot{\phi}$. It is to be noted that the phase relation is small or negligible. The reason the larger instrument volume at the higher angular frequency does not even allow a pressure transmitting tube is because of the high impedance at the entrance to the instrument volume controls conditions in the tube, and the theory fails.

A study was made of several types of pressure recording instruments to determine the instrument volumes. Since the pressure transmitting tube volume in the model is limited from 0.0001 to 0.0005 in^3 by the limit on allowable tube inside diameters, determined by the allowable subtended arc and the model diameter, very stringent requirements are imposed upon the allowable instrument volumes if high quality pressure transmission is to be attained. Only certain types of transducers or piezometric crystals located in the body, and rotating with the body, or having a properly designed rotating seal could be used to continuously measure the pressure. These will be discussed later.

B THE PRESSURE PULSE SAMPLING METHOD

In an effort to avoid the severe requirements on instrument volume and to reduce or eliminate the problems of determining the phase lag, it was decided to abandon the continuous sampling method, and to investigate the possibility of pulse sampling. Figure 4 is a diagrammatic sketch of the components involved in the pulse sampling method. The rotating body is represented by the thin-walled circular cylinder, CDE. A pressure transmitting tube or orifice is shown at C. The inner wall of the cylinder is honed to a high finish. A pressure pickup (segment of a slip ring) is spring mounted, and makes bearing contact with the inner wall along the arc, AB. The pressure pickup is mounted in a clamped trunnion at F so that it may be located circumferentially around the body. A hole drilled in the pressure pickup is connected to a manometer, M. When the orifice is located at D so that it is mating with the hole in the pressure pickup, the pressure on the outside of the cylinder is being compared with the pressure in the manometer. Any difference of pressure will cause a small amount of fluid to flow in or out of the tube. This flow is the pulse. As soon as the orifice rotates away from D, the pressure in the manometer is sealed off by the bearing contact along the arc, AB. If the seal were perfect and the pressure on the surface of the cylinder at D did not change, the repeated pulses to the manometer would adjust the pressure in the manometer equal to that at the surface at D minus the pressure change along the pressure transmitting tube due to the radial acceleration if acoustical and phase lag effects can be neglected.

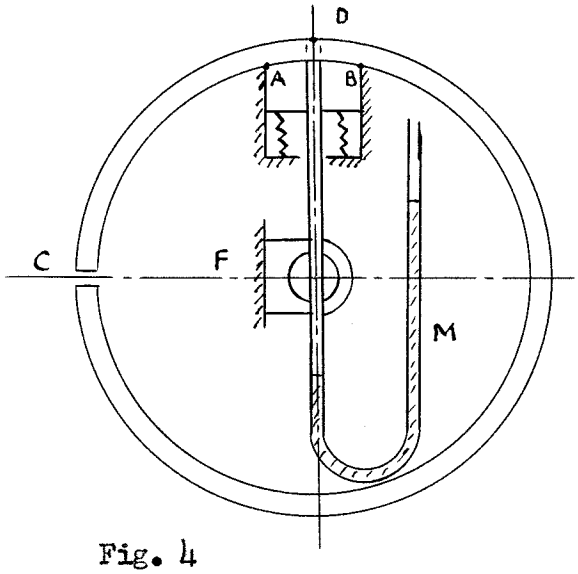

Fig. 4

However, there will be leakage in or out of the manometer along the bearing contact arc, AB, since a perfect seal can not be made. Thus, in the time interval between pulses, there will be a change of the pressure in the manometer. If the seal can be made good enough and the characteristics of the leak can be determined, the loss of pressure can be calculated. When equilibrium conditions have been attained, the average pressure between pulses can then be determined, and a correction factor applied to determine the true pressure.

Upon examining the conditions of flow along the bearing arc, AB, one sees that the flow in a circumferential direction between the pressure pickup hole and the edges A and B is similar to the flow in a viscosity pump, while axially it is similar to Poiseuille flow with a superimposed Couette flow at right angles. The pickup orifice behaves like a source or sink, and the Couette flow like a free stream, and the combined flow similar to a source in a uniform flow. The main flow of the leak might be expected to be contained in a circumferential channel, with the rotating body acting like a viscosity pump. It is known that the volume rate of flow through a viscosity pump is proportional to the pressure head opposing or aiding the flow, so one might conclude that the quantity rate of flow out or into the manometer per unit time ought to be proportional to the pressure difference between the manometer and the pressure at the edge of the seal along the bearing arc, AB. The rate of change of pressure in the manometer ought to be proportional to the pressure difference across the seal. A static test was performed to determine static sealing characteristics: the rate of leakage, the effect of bearing pressure, length of sealing path, eccentricity, and total bearing area.

It was found that due to the difficulty in preparing large surfaces uniformly smooth and plane that the larger areas tested did not give repeatable data, while the smaller areas gave excellent results. The finish on the small areas appeared to be more uniform and smoother, but the porosity of the carbon used for the sealing material would limit all blocks to the same finish. It was found that the rate of change of pressure varied inversely as the leak path length and the bearing pressure, up to a bearing pressure of 30 pounds per square inch above which little improvement was found. The time for the pressure difference across the seal to decrease to one half the initial applied pressure difference, called the relaxation time, was found to be approximately 100 seconds per linear inch of leakage path per pound per square inch of applied bearing pressure per cubic inch of trapped gas, using a polished brass surface and carbon blocks for the sealing material. These results are tabulated in the data. Carbon was selected as a bearing material because of its excellent wearing properties, ease of machining, lack of need of a lubricant, freedom from seizing at higher temperatures, and the trouble free experience of the use of carbon brushes in electric motors.

Using the above information, one can readily compute the expected average pressure to be obtained from a multiple orifice-seal pulse sampling pressure pickup. The differential equation is

$$d(\Delta p) = -\lambda(\Delta p)\, dt \qquad (20)$$

where λ is the decay constant equal to $0.693/T_{\frac{1}{2}}$ for exponential decay, and (Δp) is the pressure difference across the seal at the time t. $d(\Delta p)$ is the amount the trapped pressure has leaked in the time dt.

This equation has the following solution:

$$\Delta p = \Delta p_o \, e^{-\lambda t} = \Delta p_o \, 2^{-t/T_{\frac{1}{2}}} \quad , \qquad (21)$$

where Δp_o is the pressure difference across the seal the instant the orifice closes, and $T_{\frac{1}{2}}$ is the relaxation time. One may readily show that the average trapped pressure is

$$\overline{\Delta p} = \frac{\Delta p_o T_{\frac{1}{2}}}{0.693 T}\left[\frac{2^{T/T_{\frac{1}{2}}} - 1}{2^{T/T_{\frac{1}{2}}}}\right] \quad , \qquad (22)$$

where T is the time interval between successive orifices. That is,

$$T = \left[\frac{2\pi - 2nd/r_I}{n\dot{\phi}}\right] \qquad (23)$$

where $\dot{\phi}$ is the angular velocity of rotation, n is the number of orifices on the inner perimeter, d is the diameter of the orifice, assumed small compared to the diameter of the body, and r_I is the inner radius of the body.

If one defines :

$$K(\dot{\phi}) = \left\{\frac{0.693\ (2\pi - 2nd/r_I)}{n\, T_{\frac{1}{2}}\, \dot{\phi}}\left[\frac{2^{T/T_{\frac{1}{2}}}}{2^{T/T_{\frac{1}{2}}} - 1}\right]\right\} \qquad (24)$$

and utilizes equation (2a), then for an incompressible fluid the true pressure at the surface of the rotating body in terms of the measured pressure difference at the manometer, $(\overline{\Delta p})_m$, since a manometer is an average measuring device, is

$$p = p_a + (\overline{\Delta p})_m K(\dot{\phi}) - \rho_a \dot{\phi}^2 \left[r_o^2 - r_I^2\right] \qquad (25) \ ,$$

where $\rho_a \dot{\phi}^2 \left[r_o^2 - r_I^2\right]$ is the increment of pressure due to the radial acceleration. The function $K(\dot{\phi})$ has been calculated for the designed model having 4 orifices of 0.025 inch diameter for the design range of $\dot{\phi}$ of 20π to 200π radians per second and assuming $T_{\frac{1}{2}} = 1$ second.

TABLE II					
$\dot{\phi}$	20π	40π	60π	80π	100π
$K(\dot{\phi})$	1.0171	1.0085	1.0057	1.0043	1.0034

It is seen that using a pessimistic value of $T_{\frac{1}{2}}$, equal to 1 second, for the dynamic condition gives a measured average pressure difference which allows for leakage, of less than 2% of the applied pressure difference expected to be stored at each pulse. This, combined with the very small difference due to the radial acceleration of approximately 0.2% means that the uncorrected pressure difference should be within 2% of the correct value over the full range of testing $\dot{\phi}$. If acoustical effects do not cause serious trouble, and if the seal can be made to function properly, the pressure pulse method offers a very attractive solution to the problem of measuring the pressure distribution on a rotating body.

Part II - PROPERTIES OF PRESSURE SENSING ELEMENTS AND EFFECT ON MODEL CONFIGURATIONS

A - DESIGN REQUIREMENTS

The design requirements for the measurement of the pressure distribution on an axially symmetric rotating body are as follows:

1. The existence of small compact pressure elements which can sense the pressure at a point on the surface of the body without interfering with the external flow, and which is not sensitive to vibration, radial acceleration or acoustical effects.

2. The means of accurately locating the point on the surface at which the pressure is being measured with respect to a body fixed set of axes. Location must be both axially and circumferentially.

3. The angular frequency must be accurately measured.

4. A method of rotating the body which does not interfere with the pressure measurement, either by restricting the usefulness of the pressure pickup, or by introducing extraneous perturbations into the external flow field.

5. A method of providing structural support which will not interfere with, or restrict, the pressure measurement or the rotating mechanism, and is free from vibration and has small deflections in any attitude.

6. Means must be provided to align the model with the free stream flow both in yaw and pitch.

7. The device shall require the minimum of external equipment for sensing and recording data obtained from the model.

8. The device shall be simple, easy to maintain and adjust.

9. The device shall use existing equipment whenever possible, and be interchangeable with the existing Galcit "Magnus Effect" investigation equipment, so that it may be used for other research currently in progress, and must fit in the test section of the Merrill Tunnel.

B ADVANTAGES AND DISADVANTAGES OF POSSIBLE USE OF VARIOUS PRESSURE SENSING ELEMENTS AND THEIR EFFECT ON MODEL CONFIGURATIONS

There are several methods by which the static pressure may be sensed on a rotating body depending upon the characteristic of the element and the auxiliary equipment required to measure and record the data. There are model configurations inherent in the choice of any one sensing element. Some of the sensing elements are: a piezometric crystal, a pressure transducer, and a manometer. These will be discussed in turn.

1. Piezometric crystals.

Considerable progress has been made in aerodynamics in the application of piezometric crystals as pressure sensing elements. They can be made small and compact, and are admirably suited for the measurement of rapidly fluctuating and transient phenomena, and are ideally suited to continuously sampling on a rotating body. They are capable of extremely sensitive measurement of small pressures to very large pressures, can withstand considerable shock and have no moving parts. The crystal is sensitive to vibration, acceleration, electrical, and thermal effects. In the model these are all variables, and some are completely unknown, but presumably the crystal could be calibrated for these effects. However, the radial accelerations alone would vary from approximately 4 to 400g in the expected range of operation. This would correspond to an equivalent pressure of from 0.03 to 3 pounds per square inch, while the peak aerodynamic load in a 100 m.p.h. cross flow would be only 0.53 pounds per square inch. At small angles of yaw, the aerodynamic load would be small compared to the radial acceleration. The aerodynamic data would be obtained by taking the difference between two large numbers which would leave considerable doubt as to the accuracy of the data.

The crystal could be mounted flush with the surface of the body, and thus eliminate the pressure transmitting tube with its attenuation and phase lag problem. However, in order to obtain a reasonable electrical signal, the crystal should be approximately one half inch in diameter in order to measure small pressures.

This would correspond to a subtended arc of 19° on the surface of the model. The pressure measured would be the average pressure over the 19° of arc. With the large pressure gradients known to exist from classical theory, such a pressure reading would be meaningless. In order to average the pressure on the surface of the model over a small subtended arc, the crystal would have to be mounted in an insulated capsule inside the body as shown in figure 5. Due to small pressure transmitting tube volume, the allowable instrument volume, determined from Table I, would permit only 0.020 in. clearance between the outer face of the crystal and the mounting chamber. This may introduce some spurious acoustical effect. Because of the high rotational speed, the crystal mounting would require mass balancing of the model by using a dummy installation at 180°. This further reduces the usable internal volume for structure. Since the crystals are fixed and axial spacings of the order of one inch are desired to give axial pressure gradients, alternate pairs would have to be mounted 90° apart. In a three inch diameter model the depth of the crystal and its mount would require approximately one half inch, and when one considers the width of the mount, this leaves approximately 1½ to 1-3/4 inch diameter in the center of the body for structures, driving mechanisms, slip rings, and to bring the electrical leads out of the model. The crystal requires a cathode follower to be mounted as close to the crystal as possible, and an amplifier with a flat response from 15 cps to 100 kilocycles. It would be desirable to have the cathode follower mounted internally and rotating with the crystal.

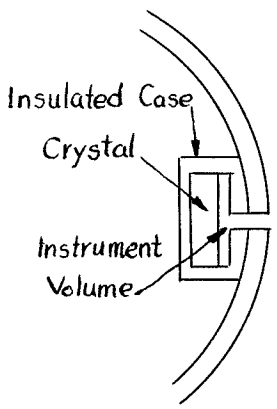

The signal could then be brought out of the model through slip rings and amplified externally. Unfortunately, the cathode follower, unless miniaturized equipment were used, would be larger than the diameter of the model. This would require that the cathode follower be mounted in the rear mounting support of the model, and the weak signal from the crystal brought out of the model through the slip rings.

Since continuous sampling would be used, a recording oscilloscope would be required. With from 15 to 20 axial stations being used on the model, and since only one crystal could be recording at a time, a rather elaborate electronic switching system would be required to record data from each crystal in turn. As a minimum of 2 leads per crystal would be required, a rather large cable, which would have to be brought of the model, would result.

In order to locate the position of the crystal as it rotates, a pulse generator mounted on the model and synchronized to the position of the crystal would have to be used. Using an oscilloscope, accurate positioning and r.p.m. can be measured.

The method of supporting and driving the rotating part of the model would seriously tax the ingenuity of the designer. To reduce vibration due to mass unbalance, the supporting bearings should be as far apart as possible. This could be achieved, but a conflict arises with the method of driving the rotating body. It may be assumed that this can be solved.

In summary, while the piezometric crystal looks attractive, the problem of attenuation and phase lag is not eliminated, since the crystal must be mounted internally, the sensitivity of the crystal to vibration, acceleration, thermal, and electrical effects, the method of obtaining

the data coupled with the problems of bringing the signal out of the model, and providing auxiliary recording equipment, and at the same time being able to give adequate structural support make the piezometric crystal an expensive and doubtful pressure sensing element in this application.

2. Pressure Transducers.

Strain wire pressure transducers offer another possibility of sensing and transmitting a pressure signal from the surface of a rotating body to a recording device. They eliminate the cathode follower, are relatively small, compact instruments, and can be obtained commercially with a wide range of sensitivities. They could be mounted radially or axially, and may rotate with the body or be stationary. If stationary, a sealing problem arises which complicates the measurement problem, but simplifies the structural and driving problem. These will be discussed in turn. Figure 6 is a diagrammatic sketch which illustrates the methods of mounting and the complications which arise.

a. Rotating Transducers.

1. The radially mounted rotating transducer, figure 6a has all problems of the piezometric crystal, and because of their larger physical dimensions, the structural and driving problems are more severe. In fact, the smallest transducer commercially available if mounted radially would allow no internal structual support within the limited diameter of the model. The rotating body would have to support all loads as a cantilever beam mounted on two bearings at the rear. The bearings could have only a limited axial spacing, and with normal bearing tolerances would allow considerable vibration. The model would be extremely difficult to mass balance because of the asymmetries in the mass distribution of the transducers.

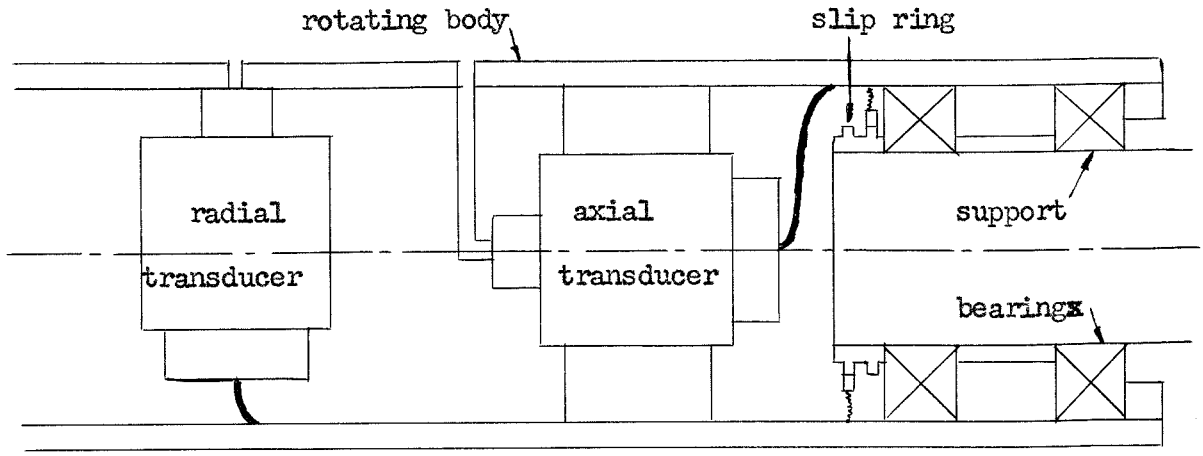

6a 6b

rotating transducers

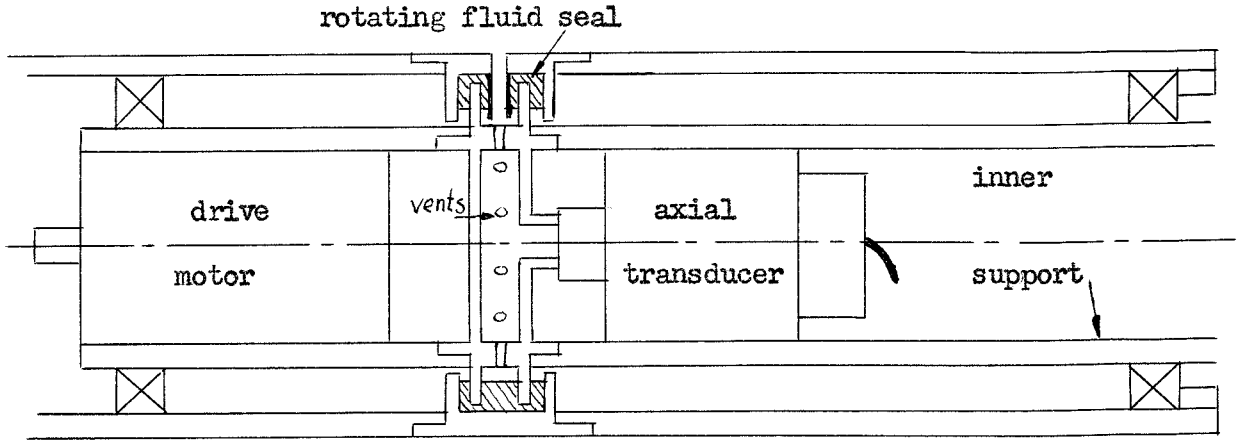

6c stationary transducer

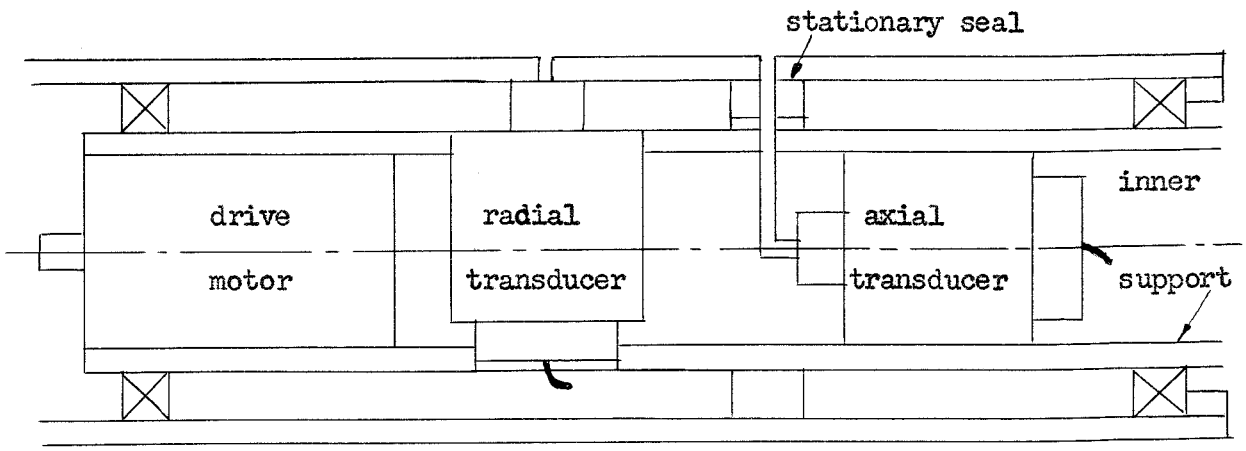

6d 6e

stationary pulse sampling transducers

Fig. 6

This would magnify the vibration problem. The slip rings would have to be at the bearing end of the model instead of distributed axially as there is no internal support. This would make assembly difficult, and means would have to be provided for retracting the brushes during assembly.

2. The axially mounted transducer, figure 6b, would eliminate some of the problems of mass balancing and vibration, and eliminate the sensitivity of the transducer to radial acceleration and transverse vibrations. However, the effect of radial acceleration on the pressure attenuation and phase lag are now magnified. All the rest of the problems remain.

b. Stationary Transducers.

1. In an effort to introduce internal structure to reduce the vibrational problem by providing a large spacing for the bearings, to relieve the rotating body of carrying any loads, and to eliminate any spurious effects on the transducer because of its rotation and lateral vibrations, the scheme in figure 6c was investigated. This was an axially mounted continuously sampling transducer. This necessitated the introduction of a rotating seal between the rotating outer body and the stationary inner body, and a sealed pressure chamber leading to the transducer. The rotating seal was designed to be packed with grease, or filled with fluid carried by tubes on the rotating body from a slinger ring which could be filled when the model is running. The fluid could be removed before stopping the model by a scoop system in the slinger ring. When the seal is full, the pressure transmitting tube protrudes above the surface of the fluid or grease into an annular chamber bounded by the surface of the fluid, the inner body, and two fins screwed to the inner body.

This chamber would be vented to an inner pressure chamber at the face of the transducer, or have a single tube leading to the transducer from the annular chamber. The fluid is contained in a circular channel formed by the fins attached in an alternate manner to a succession of cylindrical rings which formthe outer body. This arrangement requires that the rotating body and the inner support structure be a series of cylindrical tubes screwed together in a definite sequence. Once assembled no axial motion could be tolerated. Only a limited number of stations could be assembled in this way, but to obtain more axial stations, a set of cylindrical inserts could be inserted between the nose piece and the outer rotating body. In this manner complete axial coverage could be obtained. The motor is placed at the nose end of the internal support, and solves the drive problem. A short quill shaft connects to the nose piece. A bearing is placed at the nose end of the internal support and the tail end of the model to give a large bearing separation.

This configuration appeared to satisfy most of the design requirements, but to have several very undesirable features. The design of the inner body and the outer body was extremely complicated, and would not lend itself to easy maintainace of the seal, bearings, motor, or transducers. The greatest objection was that a single pressure transmitter tube must be used to connect the surface of the model to the annular chamber, which in turn was vented to the inner chamber through several orifices or by a single tube to the face of the transducer. This meant a large instrument volume, and since the signal from the pressure transmitting tube would have to travel in an arc to reach a vent or the tube to the transducer undesirable acoustical and phase lag could occur.

These problems of phase lag and signal attenuation are beyond analysis, and all the problems and equipment for continuous sampling remained.

2. It was a conceptually difficult step to abandon the continuous sampling method and change to the pulse sampling method when it appears so obvious. There was a theory for continuous sampling, and none for pulse sampling. The concept of pulse sampling arose from trying to simplify the sealing and structural problems associated with the stationary transducer discussed in 1. The idea of using a slip ring with a brush which picked up the pressure pulse immediately suggested that the transducer be placed radially to conserve space and improve the number of axial stations which could be sampled. It also suggested that the transducer be placed axially as shown in figure 6e. The pulse method eliminated the need for timing pulses and hence the oscilloscope. The position of the point at which the pressure was being measured could be accurately determined by using the inner body as the journal of a bearing, and placing a protractor on the stationary part. Relative motion was provided, and a simple clamp could hold the inner body stationary at any given circumferential orientation or azimuth angle. The axial location is known from the location of the orifice, and inserts could be used to vary the relative axial position. In addition, the structure could be made continuous which would aid in obtaining rigidity. The pressure could be measured by the use of a simple milli-voltmeter and eliminate much costly equipment.

3. Manometers

Once the concept of a pulse sampling device had been achieved it was a simple step to go from electrical recording directly to use of a manometer. The voltmeter and manometer are essentially average reading instruments.

Since to use the stationary transducer, pressure must be transmitted across a seal, the only advantage to the transducer is that it may be simpler and more trouble free to bring an electrical lead out of the model as there is less likelihood of an electrical short at the low voltages used than a pressure leak. On the other hand, the manometer allows direct measurement of the pressure, and does not need to use an intermediate device with its additional calibration and conversion factor. Also, the pressure signal may be relatively stronger than the electrical signal, and is less likely to pick up extraneous noise from the drive motor.

In using manometers, one merely uses the concept of pulse sampling described in Part I, uses the stationary transducer configuration of figure 6d or 6e, eliminates the transducer, and brings the pressure lead out of the model by passing it down a tube on the axis of the body. Rather than have a series of seals, one can hone the inner surface of the outer body to make one large slip ring, and make the pressure pickup so that it can be moved axially from pressure orifice to orifice. This introduces a minor axial location problem.

Part III - DESCRIPTION OF THE FINAL MODEL

The design of the final model was based upon the pulse sampling method using a manometer to measure the pressure directly. It went through many evolutionary changes as each new system was introduced into the model. The initial model was to be one designed for two dimensional testing only, to prove the feasibility of the pulse sampling method. The components of this model were to be designed so that they could be utilized in a three dimensional model, so as to save time and money. As the various systems were introduced into the design, it became apparent it would be less costly, and save time and money to design the three dimensional model from the start. In order to insure that the effort would not be wasted if the pulse sampling method did not work, the model was designed so that it could be used also for boundary layer research with the hot wire anemometer. The two dimensional test program could be conducted with the three dimensional model to prove the pulse sampling method, and determine the essential features of the pressure distribution on a two dimensional rotating body. The two dimensional testing could be conducted in a special diffuser which could be attached to the exit of the Galcit Boundary Layer Tunnel. The three dimensional tests were to be conducted in the CIT Merrill Tunnel, and the size of the test section of the Merrill Tunnel put a limit on the size of the model. This put a serious restriction on the design of many of the components which could have been solved easily if the model could have been larger. A satisfactory solution was obtained by designing and manufacturing special equipment for the model.

The final configuration of the model will be described, and a discussion of the design features and compromises made will be given. Drawings of the assemblies are included to illustrate and clarify the discussion. Complete working drawings of all parts are on file in the Galcit Aero. Machine Shop.

A - SYSTEMS IN THE MODEL

The model is composed of the following systems:

1. the aerodynamic envelope,
2. the pressure pickup system,
3. orientation and location of the pressure pickup,
4. r.p.m. measurement system,
5. motor drive system,
6. model internal support and structures,
7. model mount and yaw orientation system.

B - DISCUSSION OF THE SYSTEMS

1. The aerodynamic envelope has a fineness ratio of ten. The nose has a length of 3 diameters, and is one half of a prolate ellipsoid. The after body is a circular cylinder, and has a length of 7 diameters. The rear supporting tube, which is stationary and has a length of 4 diameters, is an extension of the after body, but separated by a gap of approximately $\frac{1}{4}$ of an inch. The rear support tube enters the rear support housing one diameter from the base of the rotating forebody. The rear support housing has a length of 2 diameters, and a diameter of 7/6 of the rotating body diameter. The housing has a conical taper of 1:12 in the first $\frac{1}{2}$ diameter of its length.

2. The pressure pickup system consists of the pressure pickup head and its radial bearing pressure control rod (axial tension rod), and the outer body with its orifice system (pressure transmitting tubes). The outer body (cylindrical section of the aerodynamic envelope) is a 3.000 inch diameter tube 21 inches long. The tube is made of X4130 steel, and the outer surface is polished while the inner surface is concentric to 0.0002 inch and honed to a surface finish of 10 micro-inches. There are 17 rows of orifices of 0.025 inch diameter drilled through the body with an axial spacing of one inch. The orifices start 1-3/4 inches or 7/12 diameters from the end of the nose ogive. There are four orifices in each row, and are circumferentially 90° apart. Axially the centers of the orifices on the outer surface lie within 0.001 inch of a plane perpendicular to the axis of the outer body. Because of the difficulties in drilling these holes, the centers of the orifices lie within 0.005 inch or 1/5 of an orifice diameter on the inner surface. A small axial slot in the carbon block, visible in figure 7, is 3 pressure orifice diameters in length and allows for the non-coplanarity of the orifices and any misalignment of the carbon blocks with the orifices due to variance in drilling or other sources of error. This insures that the pulse from each orifice will be registered. The orifices subtend an arc of 1.1° on the inner surface, consequently during each pulse the pressure is averaged over 2.2° of arc. This limit in arc was imposed by the difficulty in drilling and holding the holes co-planar.

Figure 7 is an exploded view photograph of the pressure pickup head, and shows the carbon blocks, blockholders, central body, retraction wedge, axial compression spring, central chamber, axial locator tube, axial tension tube with the two axial pressure transmitting tubes protruding from

the plug in the externally threaded end of the axial tension tube. The shims and bronze springs are visible on the side plate.

The pressure pickup head consists of two carbon block bearings supported in block holders, and restrained axially by the central body and circumferentially by a removable side plate. The side plates are removable to allow assembly. On each side plate are shims which prevent binding of the pressure pickup head in the ways during its traverse. Two bronze springs are on one side plate to prevent any chatter due to the design clearance and any additional clearance which may develop with wear.

Two pins are attached to each block holder, and extend through two holes in the floor of the block holder well to the central chamber. The heads of the pins rest upon the lower surface of the retraction wedge which is slotted to take the pins. Strong coil springs are placed concentric with the pins between the bottom of the block holder and the floor of the block holder well. These springs provide a lateral expansion of the block holders, and the force necessary to provide the required bearing pressure for the carbon seal. They also allow for lateral centering of the pressure pickup as it moves along its traverse, absorbs vibration, and takes up the wear in the system. The pins restrain the lateral motion of the block holders, and as the retraction wedge in the central chamber is moved axially by the motion of the tension rod and spring, the varying thickness of the wedge either permits lateral expansion of the block holders or retracts them, dependent upon the direction of axial motion. A micrometer screw at the aft end of the model controls the motion, and hence the bearing pressure at the seal. The axial tension spring pushes the wedge forward upon turning the micrometer screw in the counter-clockwise direction, and allows lateral expansion. The blocks may be retracted by a clockwise turning of the micrometer screw which moves the wedge

to the rear, and compresses the axial tension spring. The surface of each wedge is tapered 1:20 so that 1 inch axial motion of the wedge changes the diameter of the sealing blocks by 0.100 inch. The micrometer screw has 28 threads per inch, so one turn of the screw changes the diameter of the blocks by 0.00357 inch. The block retraction micrometer screw and end of the axial tension tube are visible at the extreme aft end of the model in figure 8.

Pressure orifices are drilled in the carbon blocks which mate with vertical hypodermic tubing 0.042 inch diameter swedged into the floor of each block holder. A glyptal seal is used between the carbon block and the block holder floor. Another horizontal hypodermic tube, swedged into the front of the base of the block holder, mates with the vertical tube. The horizontal tube passes through a vertical slot in the central body. A short piece of plastic tubing connects this tube with a length of hypodermic tubing which extends axially through the axial tension tube to the rear of the model where it may be connected to a manometer. The axial pressure transmitting tube is mounted in a small plug in the end of the axial tension tube with a loose fit. This allows ease of connecting the plastic tubing between the block holder and the axial pressure tube. Upon adjusting the position of the axial pressure tube to the proper length, a drop of duco cement holds it securely.

The pressure pickup head contains two carbon blocks each of which is a separately contained pressure pickup. Being located 180° apart, it is possible to measure the pressure differential across a diameter. This has the advantage that net forces can be determined from differential pressures, and where the pressures are small, greater sensitivity can be obtained.

Some loss of information occurs, but if one of the pressures is sufficiently large that it can be measured, the other can be determined from the differential pressure.

3. The orientation and location of the pressure pickup.

Figure 8 is an assembled view of the model with the aerodynamic envelope removed. The pressure pickup head and axial locator tube are visible in the axial slot in the inner support tube. The collet clamp and axial locator micrometer assembly are visible at the aft end of the model on the rear supporting tube. The rear support housing, ring clamp, and azimuth micrometer screw are mounted on the rear support saddle at the top of the pedestal mount. These comprise the location and orientation assembly.

The pressure pickup head has to be located axially and circumferentially in azimuth. The axial location is provided by attaching the pressure pickup head to the axial locator tube which passes through the dumbbell support of the aft end of the internal support body, through the rear supporting tube. The collet clamp is designed so that no torque can be put on the axial locator tube during the clamping operation, and the axial micrometer is similarly designed so that in screwing the micrometer in or out can not put a torque on the axial locator tube. The axial locator tube has the load due only to friction as the pressure pickup head moves in the ways, and the light compression load due to the axial compression spring and tube. A jam nut on the axial micrometer locks it in any desired position, and hence when the collet clamp is tightened, the pressure pickup head is located at a fixed distance from any point on the rear supporting tube. The axial locator tube is marked with circumferential marks which coincide with each pressure orifice on the outer body when the micrometer is placed in the middle of its travel

and the mark is aligned with the end of the collet clamp in the clamped position. Because of possible errors in adjustment, a visual check has been provided. The orifices in the outer body are turned to the plane of the azimuth of the pressure pickup. A dot of luminous paint is in each end of the axial slot in the carbon block. The paint dots are visible through the outer body orifice. The micrometer jam nut is then unlocked. The screw on the micrometer has 20 threads per inch, or 0.050 inch axial motion per turn. One half turn in either direction should make the luminous paint visible if the orifices are properly aligned. The outer body should be rotated slightly to insure proper azimuth location. One full revolution is required to check the positioning of all four orifices. A full turn of the micrometer screw in the opposite direction would make the other paint dot visible. If it is, one half turn back will be perfect alignment. The micrometer jam nut should then be tightened to lock everything in place.

The collet clamp and axial locator micrometer screw with jam nut are shown in exploded view in figure 9.

Azimuth location of the pressure pickup is much simpler. The pressure pickup slides in an axial slot in the inner support tube. The walls of the slot are plane, parallel, and axially located with respect to the centerline of the model to within 0.001 inch in its 19 inch length. The inner support tube is connected to the rear support tube through the dumbbell support, and securely locked by a radial set screw which acts as a shear pin to prevent rotation. The rear support tube can rotate in azimuth in the rear support housing. This rotation can be prevented by a ring clamp at the aft end of the rear support housing. The ring clamp is connected to the rear support housing saddle through a bow compass type micrometer screw called the azimuth micrometer.

The azimuth micrometer allows fine adjustment to the rotation of the rear support tube, and hence the azimuth of the pressure pickup. The surface of the rear support tube has axial marks every 10 degrees located at the front of the conical taper on the rear support housing. Every 30° are marked from 0° to 330°. The 0° mark is in alignment with the walls of the axial slot in the inner support body to within 0.10°. Three fine division scales with a least reading of 1° are provided on the rear support housing. These are located on the top and on either side, and are aligned at 90° from one another to within 0.10°. The scales have 10 divisions to both the right and left with the 5th and 10th division accented in length. The azimuth can be read directly by reading of the 10° mark on the rear support tube which is in the scale division, and adding the number of fine divisions. The azimuth micrometer has a total of 30° of fine adjustment, and should be maintained near the center of its travel for ease of use. Gross adjustments should be made by unclamping the ring clamp and rotating the rear support tube as closely as possible to the desired position, then clamping the clamp and using the micrometer screw to make the fine adjustment. The micrometer screw has been made weak purposely to discourage rough handling. This assembly can be replaced cheaply, while other mechanisms cannot.

4. The r.p.m. measurement system.

The r.p.m. measurement system consists of a magnetic pickup, an internally toothed wheel, and an electronic counter. The magnetic pickup is actuated by a variable reluctance path consisting of an internally toothed wheel and the steel barrel surrounding a coil with many turns of fine wire, and the permanent magnet, which forms the core, completes the circuit. Each time a tooth passes the end of the magnet and bridges the gap between the magnet and barrel, the magnetic field follows this low reluctance path.

As the gap between teeth passes the end of the pickup, part of the magnet field returns to the air. This variable field cuts the turns of the coil and generates a signal. This signal is fed into the electronic counter where it is counted. Each pulse is added, and the r.p.m. is read directly. The toothed wheel has ten teeth with a master tooth for comparison by oscilloscope methods.

The toothed wheel and the magnetic pickup are located at the front end of the axial slot and just behind the drive motor. The magnetic pickup is visible in figure 10 at the nose end of the axial slot just to the left of the pressure pickup. The toothed wheel is fitted into the joint between the nose piece and the after body of the rotating body. This system was in existence on a previously designed model. It was adopted to save money and make the model interchangeable. A photo electric system would have been prefered, but the cost prohibited it. The magnetic pickup was designed especially for this model, as no commercially available pickup would fit into the limited space, and had excessively large electrical connections.

5. The motor drive system.

The use of the moving pressure pickup and axial locator tube to position the pressure pick allowed only two solutions to the motor drive system. These were the alternate of placing the motor in the nose of the model and finding some way of supporting it and transferring the torque to some stationary member, or placing the motor in the rear, and using either an internal drive shaft or an external cylindrical shaft surrounding the after body. The internal drive shaft was ruled out from experience with the previous model. The nose position imposed the problem of providing cantilever support structure to the motor, and restricted the bearing area of the carbon blocks,

while the rear motor position imposed the solution of making the external cylindrical shaft removable to allow adjustments to the positioning and azimuth control of the pressure pickup. In addition, a planetary gear drive system would be required for an internally mounted motor. Internal mounting was necessary to avoid pressure perturbations on the model. The supporting structure for the rear mounted motor was very complicated, and required the use of axial slots to make adjustments. In addition, there was a problem of getting the pressure leads and r.p.m. electrical leads through the gear system and past the motor. The concept of axial slots for positioning adjustments led to the idea of an axial slot in the inner supporting structure for the pressure pickup in the final configuration. This permitted mounting the drive motor ahead of the axial slot in the internal support tube. The power leads could be brought down the D sections of the support tube, and out through the male member of the dumbbell support, through the side wall of the rear support tube to the model mount, and out of the tunnel.

Figure 11 shows an exploded view of the motor drive system, the internal support tube, and the axial slot. The front bearing journal and front ball bearing can be seen. The front bearing journal screws into the front end of the internal support tube and locked in position by a set screw acting as a shear pin. The motor is bolted to the front bearing journal by three machine screws, and positioned by the boss around the drive shaft. The power leads and terminal bracket are visible at the rear of the motor. The internally splined coupling, which protrudes through the hole in the front bearing journal and mates with the quill shaft,is visible at the front end of the motor.

The power leads and magnetic pickup leads, which pass through the male member of the dumbbell support, and their quick disconnects are shown in figure 12. The rear bearing and spacer are also visible.

In order to keep the cost down it was decided to use the drive motor from the previous model. This motor was two inches in diameter and $3\frac{1}{2}$ inches long and developed 40 oz.-in. of torque at 4000 r.p.m. Early test had indicated the desirability of obtaining pressure data as near the end of the nose ogive as possible. The size of the test section of the Merrill Tunnel placed an upper limit on the length, and hence diameter of the model, and the drive motor place a lower limit on the diameter of the model. In order to obtain the desired pressure distribution data, it was decided to push the motor as far forward as space would permit into the nose ogive of the largest allowable model. This put the first pressure orifice 7/12 of one model diameter from the nose ogive. The nose piece was hollowed to reduce weight, and to provide space for a small internal gear reduction gearbox. This gearbox, when used, can be secured to the front bearing journal by means of a barrel support to absorb the torque. This means that the front bearing must remain fixed on its journal, and the outer race have a loose fit to allow ease of assembly of the nose. A splined coupling fastened to the drive shaft of the motor mates with a quill shaft attached to the nose piece to transmit the torque of the motor to the rotating body. The quill shaft is short and stiff to avoid any torsional vibration being transferred to the rotating body. The large moment of inertia of the body should act like a flywheel and dampen out any r.p.m. fluctuation due to power supply fluctuations.

6. Model internal support and structures.

The rotating body is supported on two ball bearings mounted 25 inches apart on a slotted cantilever beam.

The beam is attached to the rear support tube through the dumbbell support, the male portion of which is attached to the internal support tube, and screwed into the female portion which is attached to the rear support tube. All joints are secured in place by set screws which act as shear pins. The complete assembly in turn slides into the rear support housing, and is accurately positioned by a shoe. The shoe slides out of a slot in the rear support housing and is actuated by a screw on the bottom of the housing saddle. The shoe mates with a circumferential slot cut in the rear support tube. The shoe and slot arrangement permits freedom in azimuth rotation of the rear support body with no axial motion.

The front bearing is mounted on a journal machined on a plug which screws into the front end of the rear support tube. An axial hole allows the motor drive shaft and the coupling to protrude through the bearing journal. The rear bearing is mounted on the male member of the dumbbell support, and a spacer holds it firmly against its shoulder. A retainer nut, which screws into the aft end of the rotating body, permits all axial play in the bearings to be taken up. The bearings' journals were machined concentrically when mounted on the internal support tube which guarantees freedom from misalignment. The model has very little vibration. What exists is attributed to mass unbalance. The general features of the structure can be seen in figure 8.

The concept of the slotted internal support tube arose from the necessity of having axial slots in the supporting structure to make adjustments to locate the pressure pickup in the "motor in the rear" configuration. This concept was the final step in determining the "motor in the front" configuration.

A compromise had to be made between the width of the slot necessary to obtain satisfactory bearing area for the carbon blocks, and the width necessary for structural rigidity at any attitude. The walls of the slot were added to provide torsional rigidity, and contribute greatly to the flexural rigidity. The walls of the slot are plane and parallel, and aligned with the centerline of the model to within 0.001 inch in it's 19 inch length. Calculations indicate that the internal support tube will not deflect more than 0.008 inch under the worst condition of loading under its own weight.

7. The model mount and yaw orientation.

The model mount and yaw orientation system consists of two components: the pedestal mount, and the support and yaw orientation assembly. The complete mount bolts on to a metal plate which in turn is bolted into the diffuser of the Merrill Tunnel. The pedestal mount consists of a circular column, capped by a block with side braces. The column fits into a circular boss on the base plate, and is fitted with a screw adjustment to adjust the model centerline height, and to a slight extent the model pitching angle. The upper end of the column mates with a hole in the rear support saddle. Two set screws in the rear support saddle mate with radial clearance into a circular slot in the top of the column. This allows the saddle to rotate in yaw, but to have no vertical motion. The weight of the model is carried by the saddle, which rests on the upper column block, which in turn transmits the load to the column and side braces.

The yaw orientation system consists of the rear housing support, housing saddle, two connecting struts, and the yaw plate. Pitching loads are transmitted from the saddle through the struts, which are primarily in tension, to the yaw plate.

The struts are bolted to the saddle so that the saddle and rear housing can be removed from the mount. Yaw attitude is provided by unclamping the yaw plate from the base plate, and rotating the saddle and yaw plate to any desired position. The plate is then clamped. The model can be yawed 15° to either side. A scale on the yaw plate indicates the amount of yaw to the nearest $\frac{1}{2}$°. The plate is aligned within $\frac{1}{4}$° to the axis of the model.

Part IV - TESTING PROGRAM

A - STATIC TESTING OF THE CARBON SEAL.

1. When the concept of pulse sampling had been completed, it was necessary to devise a suitable seal. The simplest seal was a slip ring formed by the inner surface of the rotating body and a "brush" to pick up the pressure pulse when the orifices were in conjunction. Since the surfaces had to be in rubbing contact, and since the allowable orifice diameter was only 0.025 inch, no lubrication could be tolerated. The success of carbon brushes in electric motors suggested carbon for the brush. The tube was to be of a hard metal to insure long life, freedom from distortion, and a highly polished surface. To obtain information of the sealing characteristics of carbon, a simple experiment was performed.

A small cylindrical test chamber of 4.8 cubic inch volume was made with a removable cap so that the volume could be varied by adding water. The joint between the cap and cylinder was a screwed joint, and was sealed with soft wax. The top surface of the cap was machined and polished, and vented to the atmosphere with an 0.025 inch diameter hole, the same as the orifices. A series of carbon blocks measuring $\frac{1}{4}$", $\frac{1}{2}$", 3/4" and 1" square were prepared with one polished surface. The carbon used was ordinary commercial fine grained, low porosity carbon.

The polished surface of the carbon appeared to be pitted with many tiny holes when viewed under a 25 power microscope, but the surface appeared fairly uniform, and of low porosity.

Figure 13 is a diagrammatic sketch of the test set-up. A is the cylindrical chamber vented to the atmosphere through a small orifice, O. A carbon block, B, with polished surface rests on the cap, C, and closes the orifice. The weight, W, was selected to provide various bearing pressures between the carbon block and the surface. A tube, T, in the side of the chamber connected to a 2 way stopcock. The stopcock could be turned so that the chamber, A, could be connected either to the manometer, M, or the pump, P.

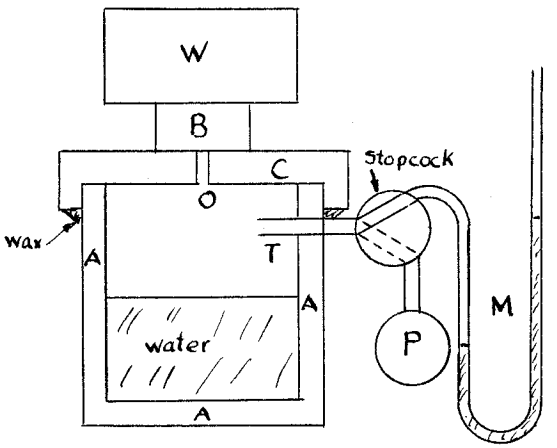

Fig. 13

The following test procedure was used: The stopcock was turned so that it connected the test chamber to the vacuum pump. The pump was turned on to evacuate partially the test chamber and put a pressure difference across the carbon block seal. The stopcock was then turned to disconnect the pump and seal off the test chamber, and the vacuum pump turned off. The stopcock was slowly turned to bleed the pressure difference into the manometer to avoid pumping fluid into the lines. When the pressure difference indicated by the manometer reached a predetermined level due to leakage into the test chamber, a stop watch was started, and pressure readings taken at periodic intervals. The slope of a curve of pressure difference versus time on semi-log paper gave the decay constant for the seal.

The time for the pressure to leak to one half the initial applied value $T_{\frac{1}{2}}$ called, the relaxation time, was taken as a measure of the effectiveness of the seal. The decay constant, λ, could also be used as a measure of sealing effectiveness, and is related to relaxation time by

$\lambda = 0.693/T_{\frac{1}{2}}$ for exponential decay.

Difficulty occured in reading both legs of the manometer simultaneously with the continuously changing pressure. It was found that, applying pressure differences as great as 30 inches of water, the manometer would adjust to this applied pressure difference in about 2 seconds with no visible oscillation. The following technique was used to insure simultaneous reading of both legs of the manometer: When the pressure fell to a predetermined point, the stop watch was started and simultaneously the stopcock closed, sealing off the manometer. Both legs could then be read in approximately 10 to 15 seconds. The stopcock was then turned to connect the manometer to the pressure chamber. The manometer immediately fell and reached equilibrium in less than 2 seconds. By selecting the time intervals of 30 seconds, for reading, approximately 15 seconds was allowed for the manometer to reach equilibrium with the slowly changing pressure. The total elapsed time for each run was 600 seconds which allowed 25 points on each curve. This gave a well defined curve and was considered to be adequate to reveal any changes in slope which might occur. Data were plotted between each run to reveal the effect of each variable as it was changed and the necessity of modifying techniques or repeating any test if in doubt.

The effect of path length was expected to be revealed by the different sized blocks, but no conclusion could be drawn from the data.

This was attributed to non-uniformity in the surface finish of the blocks and cap, variable porosity of the blocks, and the non-planarity of both the blocks and the cap. By taking any one block and moving it off center, it was found that the slope of the curve increased, and hence the relaxation time decreased. It was assumed this was due to the shorter distance from the orifice to the nearest edge of the block. Subsequent tests showed this to be true for the smaller two blocks, but with the larger blocks it depended upon the direction the block was shifted off center.

To test the effect of path length, the size of the block and the shortest path length on a given block were compared when the individual blocks were placed off center. Satisfactory agreement was obtained using the following technique. Each side of a block was marked. The block was then centered over the orifice, and scotch tape strips put on the cap along two sides of the block, but not in contact with the block. The position of all four corners were marked by an ink mark. From each corner in a direction away from the orifice, 1/16" increments were marked off. The test was started with the block centered, and then repeated each time the block was moved increments in each direction. To provide a check, the test was then repeated along a line at right angles to eliminate the effects of block and cap unevenness. This test was conducted with all four blocks at 5 p.s.i. bearing pressure, and checks were made with the smaller blocks at higher bearing pressures to see if any change occurred. Between each run, the block was lifted off the cap and placed at the new position, rather than sliding to the new position, since it was found a rather strong cohesive attraction existed between the block and plate. It also insured that the chamber came to atmospheric pressure, and a short

run of the vacuum pump was used to remove any water vapor which may have been trapped in the chamber.

To test the effect of bearing pressure, a series of weights were placed on the carbon blocks and the tests repeated. The blocks were first tested under their own weight, and then weights selected to correspond to 5, 10, 20, and 30 pounds per square inch bearing pressure. Only the smaller blocks were tested at all bearing pressures as it was found that unevenness in the surfaces of the layer blocks prevented their improvement of sealing properties with increasing bearing pressures. The smaller blocks improved up to 30 pounds per square inch bearing pressure where it fell off. This decrease in improvement was attributed to porosity, surface finish, and unevenness.

One would expect the relaxation time to be directly proportional to the volume of the trapped gas. To check this, the chamber was partially filled with water to reduce the volume by $\frac{1}{4}$, $\frac{1}{2}$, and 3/4. This was done by weighing the amount of water necessary to fill the chamber, and then adding $\frac{1}{4}$, $\frac{1}{2}$, and 3/4 of this weight. It was found the relaxation time varied directly with volume and only the $\frac{1}{2}$" block was used in this test.

To test the range of pressure differences for which the exponential decay law held, initial pressure differences as high as 30 inches of water were applied across the seal. The highest value tested corresponds to twice the highest pressure difference expected to be measured on a rotating cylinder in a cross flow of 100 m.p.h. At low pressure differences, the least reading of the manometer (0.050 inch) made readings difficult, and some scatter in the data resulted. However, tests were carried out from 30 inches of water down to 0.10inch of water, and the exponential law was verified in this range within the accuracy of the test.

The results of this experiment may be summed in the following statements: "Under the conditions of this test, the exponential decay law was verified, and a relaxation time of 100 seconds per linear inch of path length per pound per square inch of bearing pressure per cubic inch of volume of trapped gas was found. The relaxation time varied directly as the linear path length, the volume of trapped gas, and up to a limit imposed by porosity and surface planarity with increasing bearing pressure. The magnitude of the relaxation time is greatly dependent upon the surface conditions of the seal, and every effort must be made to obtain a surface of high uniform finish with uniform contour.

B--CALIBRATION TESTS OF THE MODEL

The calibration tests had not been conducted at the time this paper was prepared. This was due to difficulties in machining, certain parts had to be machined in a definite sequence. In addition, the pressure distribution model was not delivered from the contractor at the promised date. Because of the lack of time to complete the testing program, the testing program with possible difficulties to be anticipated and testing techniques are outlined in Appendix I.

APPENDIX I

CALIBRATION TESTS OF THE MODEL.

Before the model can be used for test purposes, the validity of the pulse sampling method in a controlled dynamic test has to be proved, and the characteristics of the model determined. This involves devising experiments to establish the reliability of the speed measuring system, the ability of the model to stabilize at a constant r.p.m. with and without the torque load due to the carbon blocks, to determine the lowest and highest controllable r.p.m. with and without load; to establish the variation of the relaxation time with r.p.m. and with position along the model; to establish the validity of the pulse sampling method; and to determine the range of controllable r.p.m. over which the pulse sampling method can be used.

1. Rotational speed tests.

Since the model was designed for obtaining pressure distribution data, hot wire anemometer boundary layer studies, and boundary layer transition studies, two after body cylinders were made. The pressure distribution model has 17 rows of orifices and a honed inner surface, while the boundary layer model has a polished outer surface and no orifices. Because the pressure pickup head will not be in contact with boundary layer model and will exert no retarding torque, it would be expected that the motor will be able to run at stabilized r.p.m. over a wider range of speeds than the pressure model. It accordingly will be tested first.

a. In the r.p.m. test of the boundary layer model, the assembled model will be prepared for testing. The r.p.m. control system consists of a variac transformer, a rectifier, field reversal switch, and a resistor to control the current to the armature.

In starting, the resistor in the armature circuit is cut out, and the variac output slowly increased. Since the leads to the motor are long, it will be necessary to determine the output voltage from the rectifier necessary to supply the maximum voltage of 24 volts at the terminal strip on the base of the motor. This will be accomplished by measuring the voltage at the terminal strip at the armature binding posts as torque is applied to the motor. This will be done since the line drop varies with armature current. A plot of armature current versus rectifier output voltage with no armature resistor will be obtained. The effect of an armature resistor is to reduce the r.p.m. at any given load. The r.p.m. and torque load measured will be plotted versus the rectifier output voltage. These curves show the running characteristics of the motor.

To check the r.p.m. measuring system, the magnetic pickup leads will be connected first to an oscilloscope to check the wave form of the pulse obtained from the magnetic pick up. This should resemble half a loop of a sine wave. The signal then will be fed into the r.p.m. counter to see if it needs amplification.

The armature resistance then will be cut in until the lowest speed of the model is found at which the r.p.s. does not vary more than 0.1 r.p.s. during a 5 minute running period. This will be taken as the lowest r.p.s. at which boundary layer studies can be conducted without use of the gear reduction box, which will reduce the r.p.m. by approximately 5 times due to the gear ratio and the slight torque load of the gearbox.

The r.p.s. will be increased in increments of 5 r.p.s. until the maximum r.p.s. is attained. The maximum fluctuation observed in a 5 minute running period will be observed, and plotted. This will show the stability of the model to r.p.s. fluctuation versus running r.p.s. at no load condition.

b. The r.p.m. test of the pressure model will be conducted in a similar manner to the boundary layer model, except that here care has to be taken to avoid stalling of the motor. In this test the model will be brought up to the maximum no load test speed with the blocks retracted. As the blocks are extended in small increments, the r.p.s. should be observed to slowly decrease. Stabilized running conditions of 1 minute will be allowed since the large moment of inertia of the model acts as a flywheel, and a short time interval will be required to attain equilibrium running. When the r.p.s. fluctuations of 0.1 r.p.s. are observed, the r.p.s. with load will be taken as the limit in bearing pressure allowable for satisfactory testing. This will be repeated at increments of no load r.p.s. until excessive fluctuations of r.p.s. are attained. In this manner operating boundaries for the pressure model will be obtained.

2. Determination for the Relaxation Time - $T_{\frac{1}{2}}$.

The relaxation time is expected to vary with r.p.s. and position along the tube. The variation of $T_{\frac{1}{2}}$ with r.p.s. is attributed to the allowable bearing pressure to avoid r.p.s. fluctuations, and the influence of the viscosity pump effect on the effectiveness of the seal. It is expected that $T_{\frac{1}{2}}$ will decrease linearly with r.p.s. due to viscosity pump effect, and superposed on this would be a further hyperbolic decrease with r.p.s. due to reduction in allowable bearing pressure because of the reduction of motor torque with increasing r.p.s. The variation of $T_{\frac{1}{2}}$ with position along the tube is due to any nonuniformity in surface finish, possible variations in the diameter of the inner surface, and transverse vibrations due to mass unbalance, and deviations of the pressure pickup from the center line of the model due to clearance and deviations of the slot from the axis of the model.

At any one station along the axis, the carbon block would wear to contour in time, but this would take an undue amount of time. If there is no appreciable change of $T_{\frac{1}{2}}$ along the axis, any testing program can be considerably accelerated. To determine this, the following test should be conducted.

A test set up similar to that in fugure 13 is used in which the model replaces the pressure chamber. The pressure pickup should be located half way between two rows of orifices in the lands so that no pressure pulse from an orifice is in direct contact with the mating surface of the block. The pressure lead on the front of the pressure pickup to one of the carbon blocks will be disconnected, brought around to the trailing side of the block with a given rotation and centered at the middle of the block holder. It is believed that this location will measure the greatest pressure difference across the seal. The pressure leads from the test block and the disconnected lead will be connected across the manometer. The disconnected lead measures the pressure inside the model. The motor will be brought up to no load speed, and the blocks slowly extended until stabilized running as determined in the rotational speed tests is attained. The stopcock will be turned to connect the vacuum pump, and the pump turned on. The stopcock is then turned to seal off the manometer, and the pressure slowly bled into the manometer. Using techniques similar to the static test, $T_{\frac{1}{2}}$ is determined where it is sufficiently long enough to use these techniques. Where $T_{\frac{1}{2}}$ is unduly short, the lead from the block and the manometer are attached to the stopcock by a tee fitting. The stopcock then can be connected to both the carbon block and the manometer. The vacuum pump is then turned on and a steady pressure difference applied by bleeding into the vacuum pump.

When equilibrium is attained, the stopcock is turned to seal off the manometer, and the time for the pressure to drop to zero is measured. This is to be compared with the time for the same pressure difference applied to the manometer alone to adjust to zero. The difference of the times is to be plotted versus the applied pressure difference. The slope of this curve gives the decay constant and, hence the relaxation time. Positive and negative pressure differences are used to determine if there is any effect due to flow in or out of the seal. This test is to be repeated over the useful range of r.p.s. at one station, and then repeated at several stations along the axis. The range of r.p.s. for $T_{\frac{1}{2}}$ greater than 1 sec. gives the expected range in which the pulse sampling method will have an error of less than 2% of the measured pressure difference.

3. Determination of the validity of the theory of Pulse Sampling, useful range of r.p.s., and the sensitivity of the model to measure pressure differences.

It is necessary to devise a controllable test which will prove the validity of the pulse sampling method, and the ability of the model to measure pressure differences. The sensitivity of the instrument may be considered to be determined by two factors: the magnitude of the pressure difference, and the time required for the instrument to adjust to this difference. This information must be available before a testing program can begin.

In determining $T_{\frac{1}{2}}$, the pressure inside the manometer had to be measured accurately with time. The pressure outside and inside the model did not enter directly into the test, as the pressure difference across the seal was the only important quantity.

However, in determining the validity of the pulse sampling method, the pressure in the manometer must adjust to the pressure applied by the orifices at each pulse, regardless of the pressure across the seal. The pressure inside of the model must be different from the pressure outside to verify the validity of the theory. This requires a modification of the test set up for determining $T_{\frac{1}{2}}$.

It is desirable that the test be conducted in a quiescent surrounding so that accurate measurement can be accomplished, and no extraneous currents will influence the surface pressure of the model. The pressure at the surface will then be ambient pressure and a constant. The pressure leads at the pressure pickup head will be as for determining $T_{\frac{1}{2}}$, but instead of being connected across the manometer, each will be connected to a separate manometer using ambient pressure as a reference. This allows the pressure difference across the seal and across the orifice to be determined. If the pressure in the manometer reads the same as the pressure inside the model, and is different from ambient pressure, the seal is not functioning. If the pressure in the manometer reads the same as ambient, and the inside pressure is different, the seal is 100% effective. By measuring the r.p.s., $K(\dot{\phi})$ can be determined experimentally and compared with theory. Deviations are expected, but $K(\dot{\phi})$ will become a known function.

Since the pressure on the surface of the model is ambient and constant, the pressure inside the model has to be different and controllable to verify the theory. This is accomplished in the following manner: All rows of orifices except the one used in the test are to be sealed by placing a small patch of scotch tape over each orifice. This makes the rotating

body essentially an airtight body except for leakage in through the open row of orifices, the rear bearing, and holes in the male member of the dumbbell support. The electrical lead holes are to be sealed with soft wax before assembly. The axial locator tube and hole are to be liberally coated with grease to reduce leakage to a minimum. A felt seal, is cemented just ahead of the rear bearing and on the retainer nut and saturated with oil. This allowes good sealing with low friction. These modifications effectively will seal the inner part of the model from the outside except for small leakage.

To control the pressure inside the model, the air is to be pumped out until the rate of leakage and pumping are the same. By using a high capacity vacuum pump the pressure inside the model can be lowered by as much as 150 inches of water, but tests are to be carried out using a maximum of 30 inches water. This will be effectively the pressure difference across the carbon seal. Since the axial locator tube connects the inside of the model with the outside, and carries only the lightest loads, the axial locator tube is used as a passage for pumping air out of the model. This is done by drilling two $\frac{1}{4}$" diameter holes in the walls of the axial locator tube 6 inches from the pressure pickup head, and a third $\frac{1}{4}$" hole 2 inches from the axial tension tube micrometer on the aft end of the model. Two tubes are soldered into the axial locator tube and leads to a vacuum pump connected.

The model is to be tested first in a stationery condition by sealing all the orifices and running the vacuum pump. The pressure inside the model is to be measured by using the pressure lead disconnected from the carbon block. The time to attain equilibrium for various average pressure differences, and the fluctuations about the mean will be held to 0.1 inch

of water by adjusting a needle valve to the vacuum pump. The Scotch tape over the test row of orifices then will be removed to determine the influence of the flow from the orifices. The test row of orifices is to be selected near the front end of the model to get away from eddies and pressure gradients caused by the leaks. The blocks are retracted, and the model tested in the sealed condition with the test row of orifices sealed, and then with the test row open to determine the effect of flow in the orifices on the pressure reading inside the model. The blocks then are to be slowly extended and equilibrium running conditions attained. The pressure inside and outside of the model and the r.p.s. read, and $K(\dot{\phi})$ is computed by using equation (25). The test is to be repeated using the vacuum pump as a pressure pump to find the effect of a positive pressure difference.

By steadily increasing r.p.s., a limiting r.p.s. for which the pressure pulse technique can be used can be determined. By changing the pressure difference across the seal, the limit of pressure difference for which the technique will apply can be determined.

The sensitivity of the instrument may be defined as the least pressure difference measurable at any r.p.s. divided by the pressure in the instrument, multiplies by the ratio of the time interval between pressure pulses to the time interval required for the instrument to reach equilibrium. That is,

$$S = \frac{\overline{(p)}_m}{p_I} \frac{T}{T_e} = \frac{\overline{(p)}_m}{P_I} \frac{2(-nd/r_T)}{T_e} . \qquad (26)$$

This is the average percentage change of pressure in the intrument per pulse. The sensitivity will be determined over the full range of usable r.p.s. and for a range of pressure differences. These curves will indicate the usefulness of the instrument.

Part -- VI REFERENCES

(1) " An Analytic Method for Predicting the Magnus Forces and Moments on Spinning Projectiles" , by Howard R. Kelly. U.S. Naval Ordnance Test Station TM-1634 August 1954.

(2) " Attenuation of Oscillatory Pressure in Instrument Lines", by Arthur S. Iberall. U. S. Dept. of Commerce, NBS Research Paper RP 2115, Volume 45, July 1950.

Part -- VII PHOTOGRAPHS

Part -- VIII Drawings

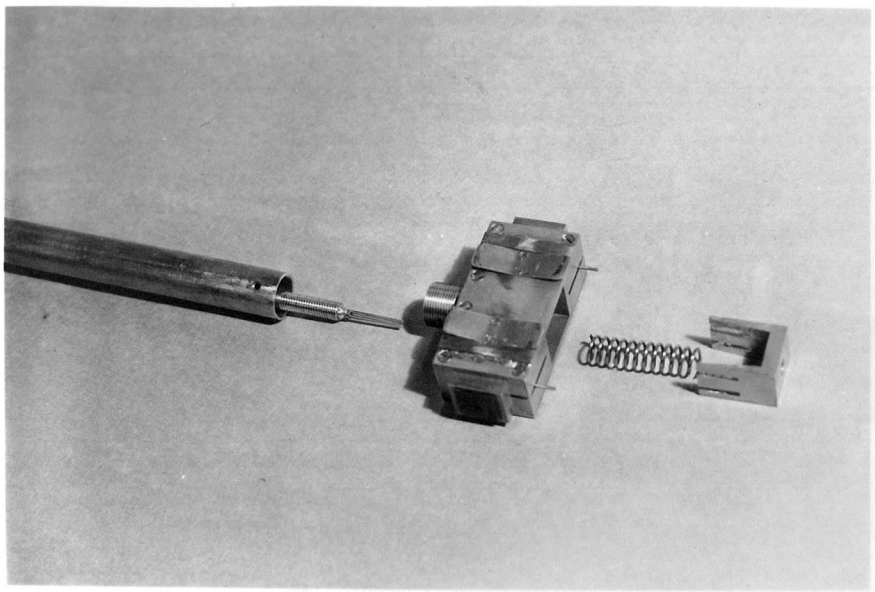

Fig. 7 Exploded View of the Pressure Pickup Head.

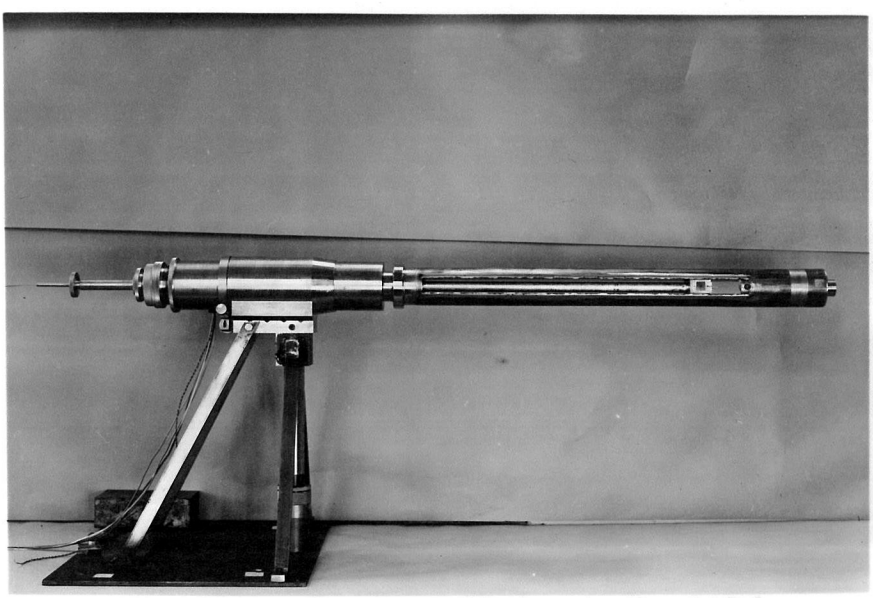

Fig. 8 Assembled Model with Aerodynamic Envelope Removed.

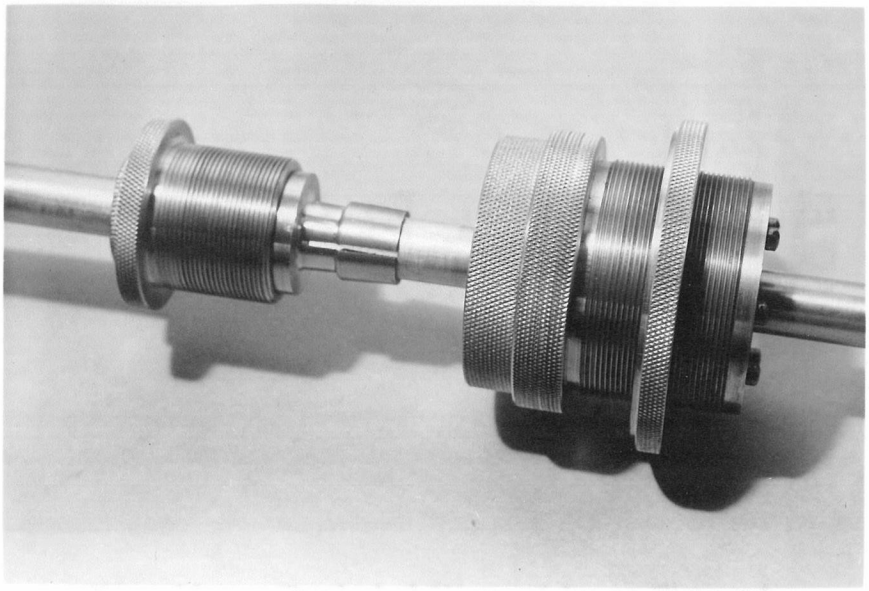

Fig. 9 Collet Clamp and Axial Micrometer Screw.

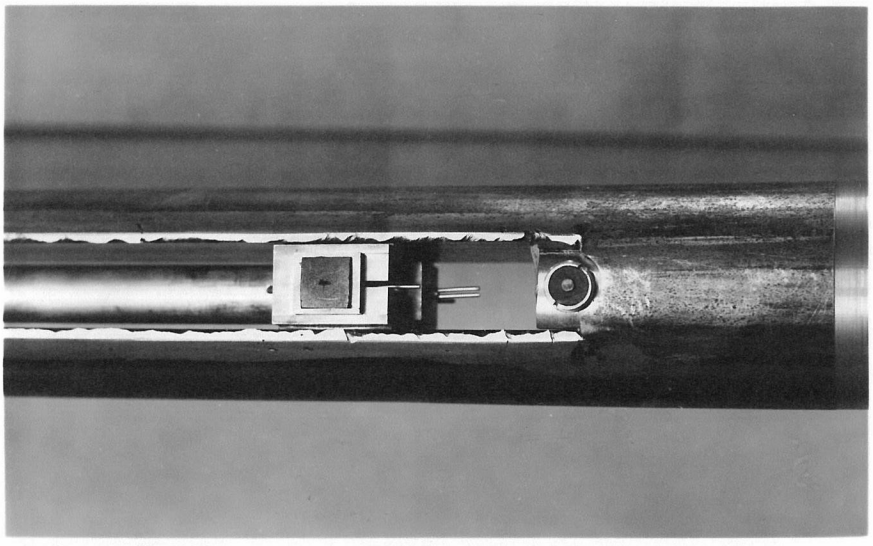

Fig. 10 Pressure Pickup in the Axial Slot, and Magnetic Pickup.

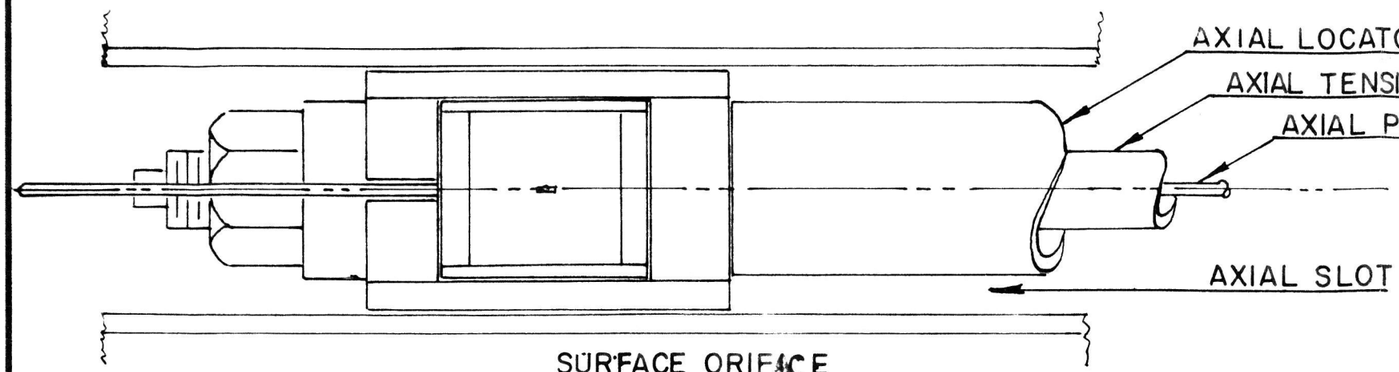

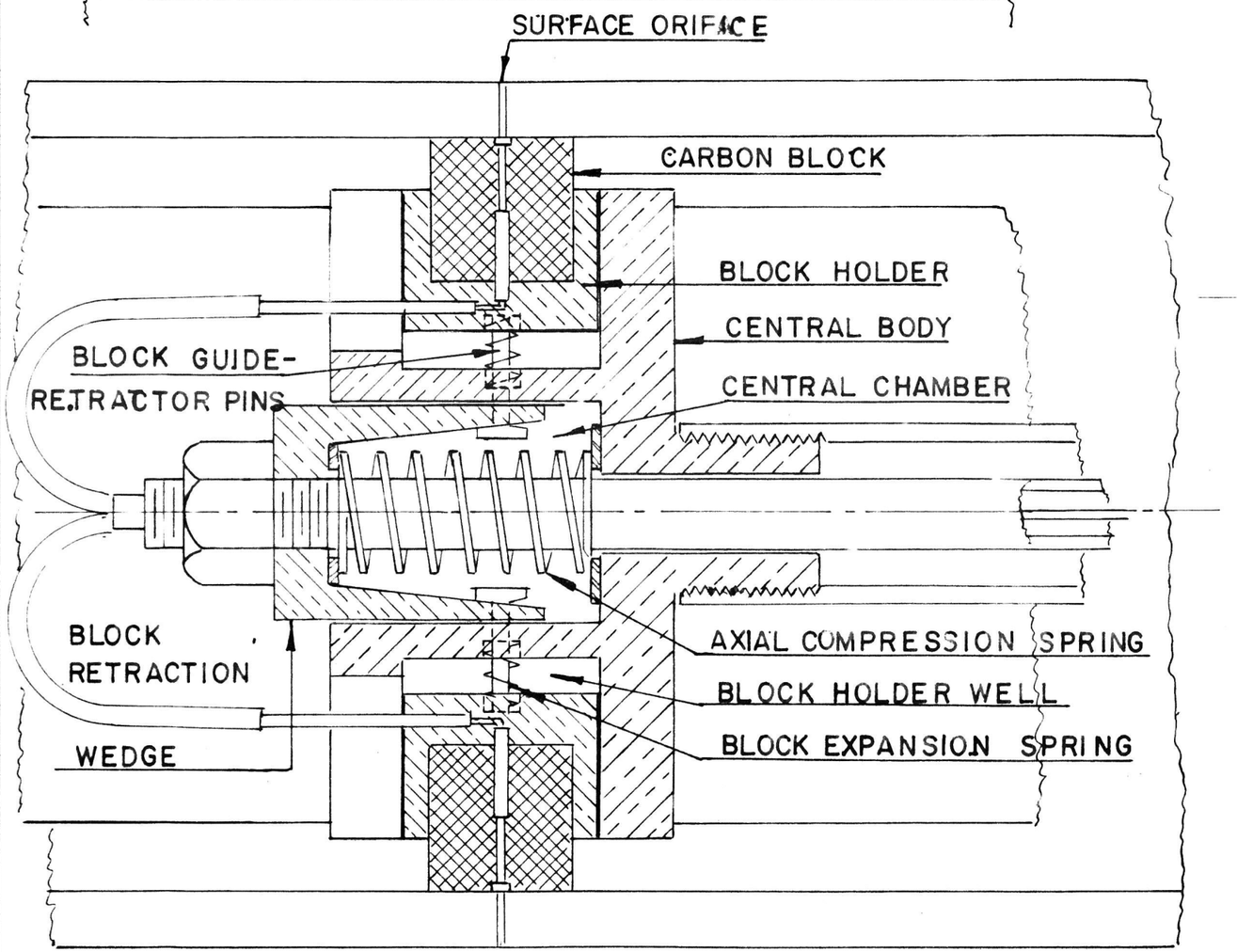

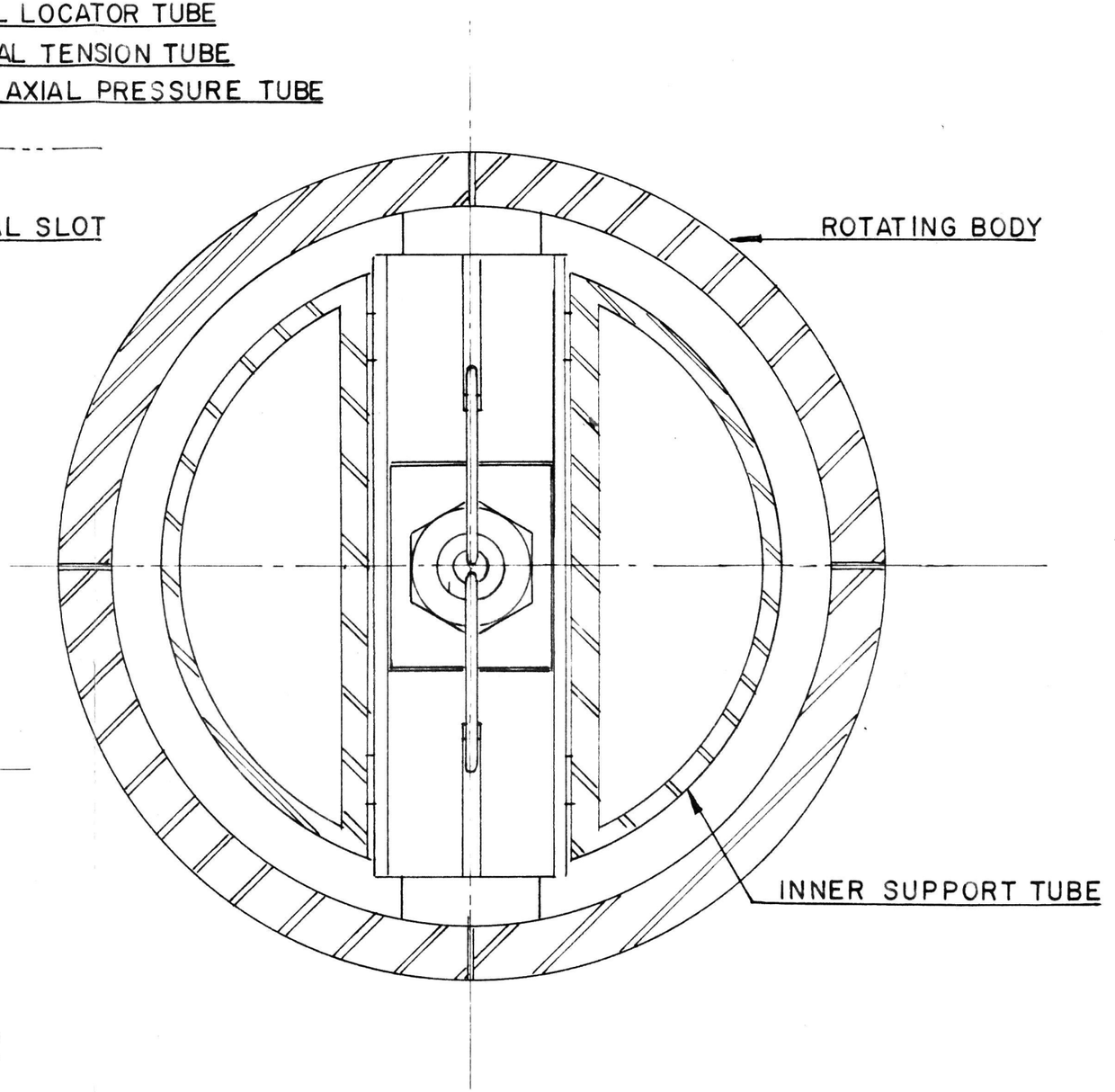

BRASS							TOLERANCES ± .010 OR ± 1/64 UNLESS OTHERWISE NOTED
			LARSEN				SCALE 2" = 1"
MATERIAL	FINISH	HEAT TREAT	DRAFTSMAN	CHECKED	APPROVED	ENGINEER	REF.
GUGGENHEIM AERONAUTICAL LABORATORY CALIFORNIA INSTITUTE OF TECHNOLOGY			PRESSURE PICKUP ASSEMBLY				55-81-3
			NAME				DRAWING NO.